

## **General Disclaimer**

### **One or more of the Following Statements may affect this Document**

- This document has been reproduced from the best copy furnished by the organizational source. It is being released in the interest of making available as much information as possible.
- This document may contain data, which exceeds the sheet parameters. It was furnished in this condition by the organizational source and is the best copy available.
- This document may contain tone-on-tone or color graphs, charts and/or pictures, which have been reproduced in black and white.
- This document is paginated as submitted by the original source.
- Portions of this document are not fully legible due to the historical nature of some of the material. However, it is the best reproduction available from the original submission.



TRW Electronic Systems Group One Space Park  
 Redondo Beach, CA 90278  
 213.535.4321

SN 39042.000  
 E130.1.83-6404

03 November 1983

National Aeronautics & Space Administration  
 Goddard Space Flight Center  
 Greenbelt Road - Building 16  
 Greenbelt, Maryland 20771

ATTENTION: Mr. Nicholas G. Chrissotimos, Code 727.2  
 Technical Officer

SUBJECT: Contract Number NAS5-26658  
 S-Band SBAW Microwave Source - Phase II  
 FINAL REPORT

In compliance with the subject contract data requirements,  
 TRW Inc., Electronic Systems Group, herewith submits ten (10)  
 copies of the Final Project Report.

If you have any questions concerning this report, please  
 contact me at (213) 535-8637, or Mail Station 138/1460.

TRW Inc.  
 Electronic Systems Group

Daniel A. Bush  
 Contracts Administrator  
 Military Electronics Division

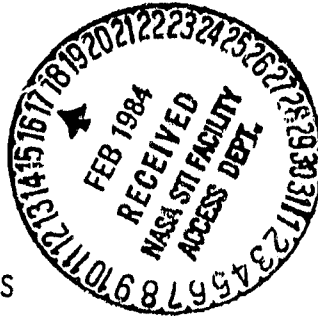
DAB/jlj

Enclosure - as stated

CC: Graphics Arts Branch (Glossy prints and negatives) - Code 253  
 Patent Counsel - Code 204 (1 copy)  
 Contracting Officer - Code 287 (1 copy)

K-F. Lau (letter only)  
 (NASA-CR-175153) S-BAND SEAW MICROWAVE N84-17432  
 SOURCE, PHASE 2 Final Report (TRW  
 Electronic Systems Group) 42 p  
 HC A03/MF A01

CSCD 20N  
 G3/32 11646  
 Unclass



CONTENTS

	<u>Page</u>
1. INTRODUCTION AND SUMMARY	1-1
2. SUMMARY OF PHASE I DEVELOPMENT	2-1
2.1 SBAW in Rotated Y-Cut Quartz	2-1
2.2 1 GHz SBAW Delay Line and Oscillators	2-4
2.3 Other Developments	2-7
3. AGING STUDY OF 1 GHz SBAW OSCILLATORS	3-1
4. 2 GHz SBAW DELAY LINE DEVELOPMENT	4-1
4.1 Devices on $36.25^\circ$ Rotated Y Cut Quartz	4-1
4.2 Devices on $-50.5^\circ$ Rotated Y Cut Quartz	4-3
4.3 Fabrication and Packaging Techniques	4-6
4.4 Electromagnetic Feedthrough	4-8
5. 2 GHz SBAW OSCILLATOR DEVELOPMENT	5-1
5.1 Detail Design	5-1
5.2 Spurious Output and Phase Noise Characteristics	5-3
5.3 Temperature Stability	5-8
5.4 Long Term Aging Characteristics	5-8
6. REFERENCE SOURCE EVALUATION	6-1
6.1 Comparison Between 1 GHz SAW and SBAW Oscillators	6-1
6.2 Comparison Between 2 GHz SAW and SBAW Oscillators	6-2
6.3 Trade-Off Between 1 and 2 GHz Reference Sources	6-2
7. FREQUENCY SELECTABILITY AND SETTABILITY	7-1
7.1 Analysis and Device Design	7-1
7.2 Data Summary	7-3

## 1. INTRODUCTION AND SUMMARY

This report describes the results of the investigation performed under NASA Contract NAS5-26658. The primary purpose of this program, entitled "S-Band Shallow Bulk Acoustic Wave (SBAW) Microwave Source," was to establish techniques necessary to fabricate a high performance S-band microwave signal source using state-of-the-art SBAW oscillator technology. The program was divided into two phases, and the present report deals with the second and final phase of this program.

The objectives of the Phase II effort were:

- Aging study of 1.072 GHz SBAW delay line oscillators.
- Development of 2.143 GHz SBAW delay lines.
- Construction and characterization of 2.143 GHz SBAW oscillators.
- Assessment of the compatibility and performance improvement of SBAW devices in oscillator circuits presently using SAW devices.
- Demonstration of a cost-effective method to produce SBAW delay line from the same mask, but operating at different frequencies.

The content of this report will follow the above outline of program objectives. A brief summary of the Phase I effort is in Section 2, which provides a background summary of the program. The results of the aging experiments on the 1 GHz SBAW oscillators are described in Section 3. Section 4 describes the design, fabrication and test of the 2.143 GHz SBAW delay lines. Two design approaches were implemented. The third harmonic transducer on  $36^\circ$  rotated Y cut quartz proved to be the most useful design, whereas the fifth harmonic transducer on  $-50.5^\circ$  rotated Y cut quartz suffered from high insertion loss and poor sidelobe rejection.

The construction and characterization of the 2 GHz SBAW oscillator are described in Section 5. Measurements included phase noise, frequency dependence on temperature, and 6-month aging. Section 6 described the comparison of SAW and SBAW oscillators. Both 1 and 2 GHz oscillators were compared. The 2 GHz SBAW oscillator showed significant improvement in phase noise and temperature stability over the 2 GHz SAW oscillator developed in previous NASA programs.

The final section describes a technique to produce SBAW delay lines of different frequencies from a single mask. The five frequencies were pre-selected within a 2.1 to 2.3 GHz range. The delay lines were incorporated into oscillator circuits to demonstrate the ability to select the frequency output of the SBAW oscillator.

## 2. SUMMARY OF PHASE I DEVELOPMENT

The five main tasks of the Phase I development were:

- Develop 1.072 GHz SBAW delay lines.
- Fabricate five hybrid 1.072 GHz SBAW reference oscillators.
- Investigate SBAW in aluminum nitride on sapphire,  $\text{AlN}/\text{Al}_2\text{O}_3$ .
- Perform a design study of the 2.144 GHz SBAW delay lines.
- Investigate SBAW delay line oscillator frequency selectability/settability.

The key element in the SBAW microwave source is the SBAW delay line. A thorough understanding of wave properties and material selection is the key to achieving good device performance. A brief discussion of SBAW theory is thus presented before highlights of the phase I activities are summarized.

### 2.1 SBAW in Rotated Y-Cut Quartz

Shallow Bulk Acoustic Waves (SBAWs) are essentially bulk waves which propagate just below the crystal surface. They can be launched and detected with interdigital transducers. SBAWs have been observed in quartz, lithium niobate, lithium tantalate and berlinite. Of these materials, only quartz and berlinite have cuts with a zero first-order temperature coefficient near the room temperature. Since berlinite is presently not available commercially, quartz was the only choice for the present application.

The SBAW in quartz has been extensively searched and characterized. SBAWs are found to propagate in singly rotated Y-cut quartz with a propagation direction at  $90^\circ$  off the X-axis. These SBAWs are pure shear plane waves with polarization parallel to the surface and perpendicular to the direction of propagation.

The wave velocity, coupling coefficient, and temperature coefficient of the SBAW as a function of the substrate angle  $\mu$  have been theoretically calculated and are summarized in Figures 2-1, 2-2, and 2-3. The angle  $\mu$  is the angle between the normal to the substrate surface and the negative crystalline Z axis. The  $\mu$  for the Y cut plate is 90 degrees.

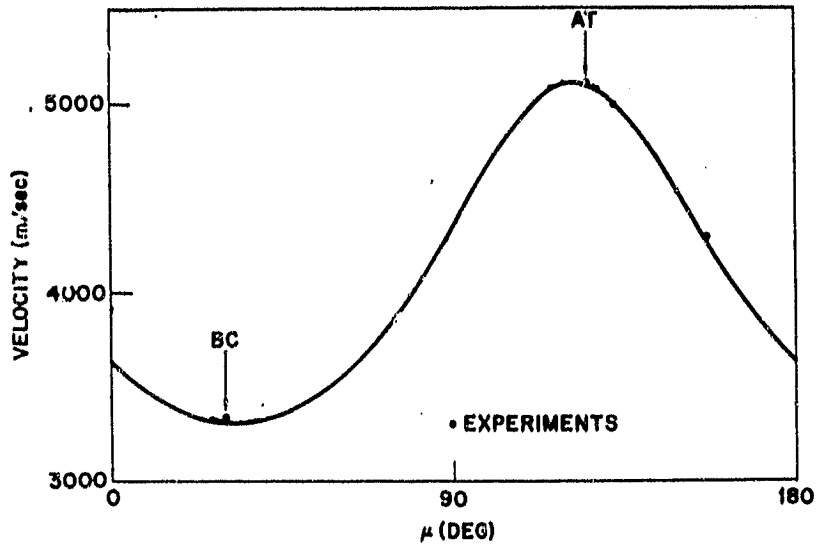


Figure 2-1. Velocity of SBAW in Rotated Y-Cut Quartz

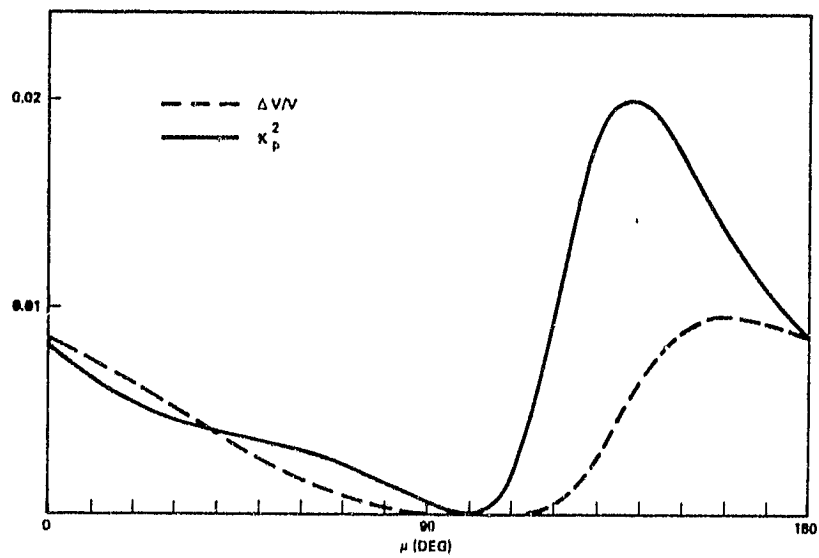


Figure 2-2.  $\Delta v/v$  and  $K_p^2$  of SBAW in Rotated Y-Cut Quartz

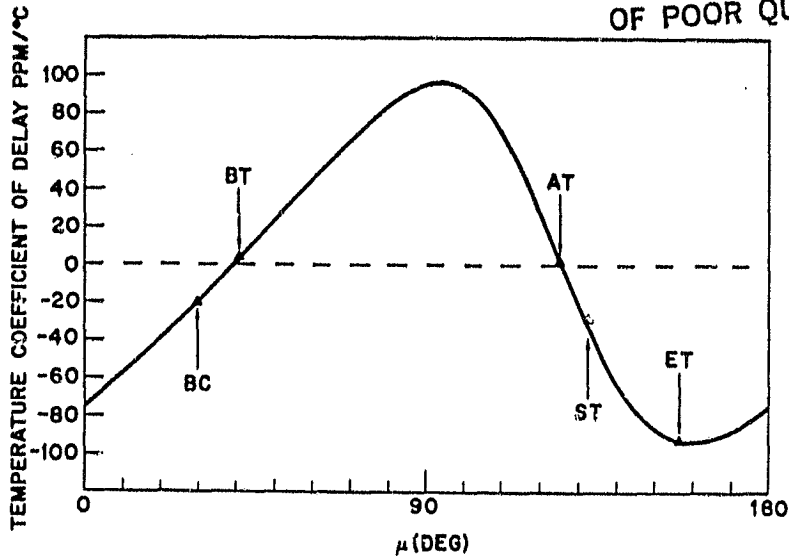


Figure 2-3. First-Order Temperature Coefficient of Delay of SBAW in Rotated Y-Cut Quartz

For oscillator applications, the SBAWs are required to be temperature stable. As shown in Figure 2-3, there are two regions of  $\mu$  where the first order temperature coefficient of delay is zero at room temperature. Specifically, the  $\mu$ 's for temperature stable cuts are  $125.5^\circ$  and  $39.5^\circ$ . According to conventional nomenclature, such cuts are  $35.5^\circ$  and  $-50.5^\circ$  rotated Y cuts. In actual devices, the metal loading effect caused by the metallic fingers shifts the temperature stable cut angles by a few degrees. The exact magnitude depends on the thickness of the metallization. These effects have been quantitatively evaluated and can be incorporated into the selection of the substrate orientation.

The comparison of the wave properties of the two temperature stable orientations is summarized in Table 2-1.

Table 2-1. Comparison of SBAW Properties Between  $+35.5^\circ$  and  $-50.5^\circ$  Rotated Y-Cut Quartz

	<u>+35.5°</u>	<u>-50.5°</u>
Wave Velocity	5100 m/sec	3331 m/sec
Coupling Coefficient	$1.44 \times 10^{-2}$	$0.41 \times 10^{-3}$
Mass Loading Effect ( $\Delta v/v$ for $t/\lambda = 0.01$ )	0.16%	0.1%
Wave Attenuation	0.83 dB/ $\mu$ sec	2.0 dB/ $\mu$ sec
Temperature Stability (-55°C to +85°C)	<u>+125 ppm</u>	<u>+55 ppm</u>

From this comparison, it is obvious that the  $+35.5^\circ$  cut has the advantage of high wave velocity, high coupling coefficient, and low wave attenuation. Its sensitivity to metal loading can also be an advantage since it provides a means for frequency trimming. The  $-50.5^\circ$  cut, on the other hand, has the advantage of better temperature stability. The overall property of the  $+35.5^\circ$  cut made it a more attractive substrate. For Phase I,  $+35.5^\circ$  cut substrates were exclusively employed.

## 2.2. 1 GHz Delay Lines and Oscillators

The basic structure of a SBAW delay line is quite similar to a SAW delay line. As shown in Figure 2-4, interdigital transducers are used to launch and detect a SBAW. Design techniques commonly used for SAW transducers are therefore expected to work for SBAW devices. During the Phase I investigation, four different designs were implemented for the 1 GHz SBAW delay line. These include fundamental thinned electrode, third harmonic, energy trapping and segmented transducer designs. The various device configurations are shown in Figure 2.5. The conclusion from this study is that while only the segmented transducer design failed to work satisfactorily, the 3rd harmonic design has the unique potential for higher frequency operation.

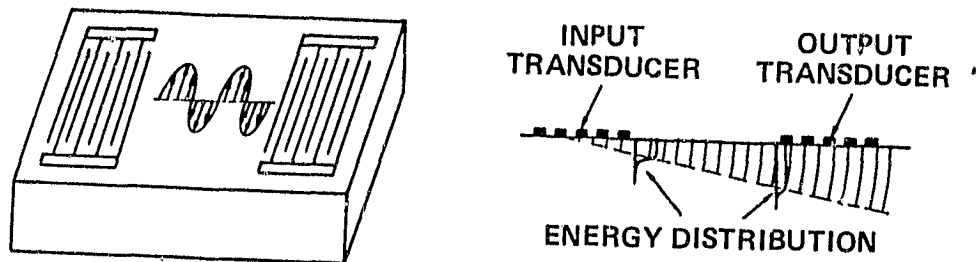


Figure 2-4. Basic SBAW Device Configuration

The third harmonic transducer thus forms the baseline approach for the 1 GHz SBAW delay line.

As shown in Figure 2-6, a typical 3rd harmonic device has an unmatched insertion loss of 26 dB, a 3 dB bandwidth of 2.28 MHz, and an oscillator Q of 1220. The minimum linewidth for the transducer finger is  $1.78 \mu\text{m}$ .

Five 1.072 GHz SBAW oscillators were developed under Phase I of the program. The schematic diagram of these oscillators is shown in Figure 2.7.

ORIGINAL PAGE IS  
OF POOR QUALITY

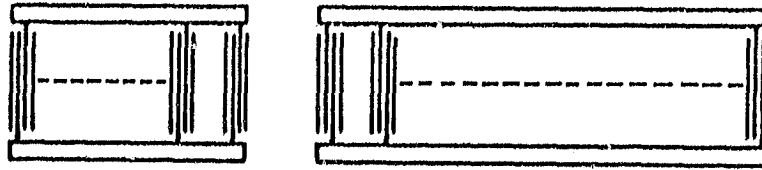


Figure 2-5(a). Thinned Electrode Transducer Configuration

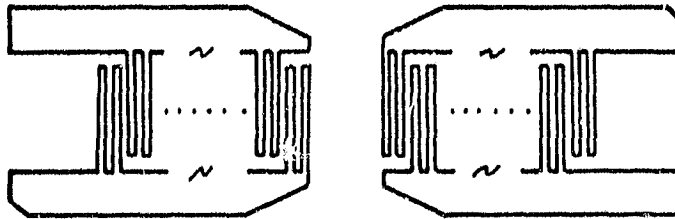


Figure 2-5(b). Third Harmonic Transducers

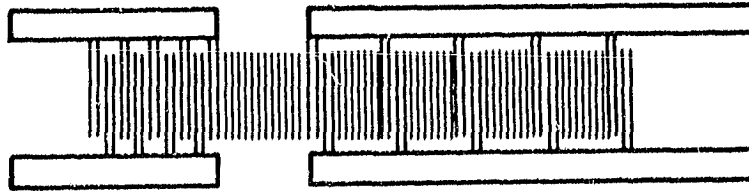


Figure 2-5(c). Delay Line Employing Energy Trappings Gratings

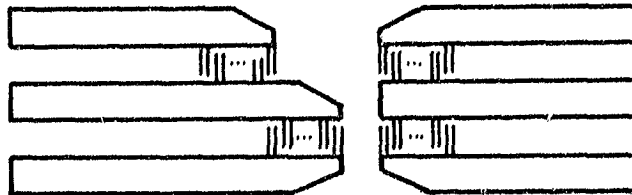


Figure 2-5(d). Segmented Transducer Design

Figure 2-5. Various Transducer Configurations

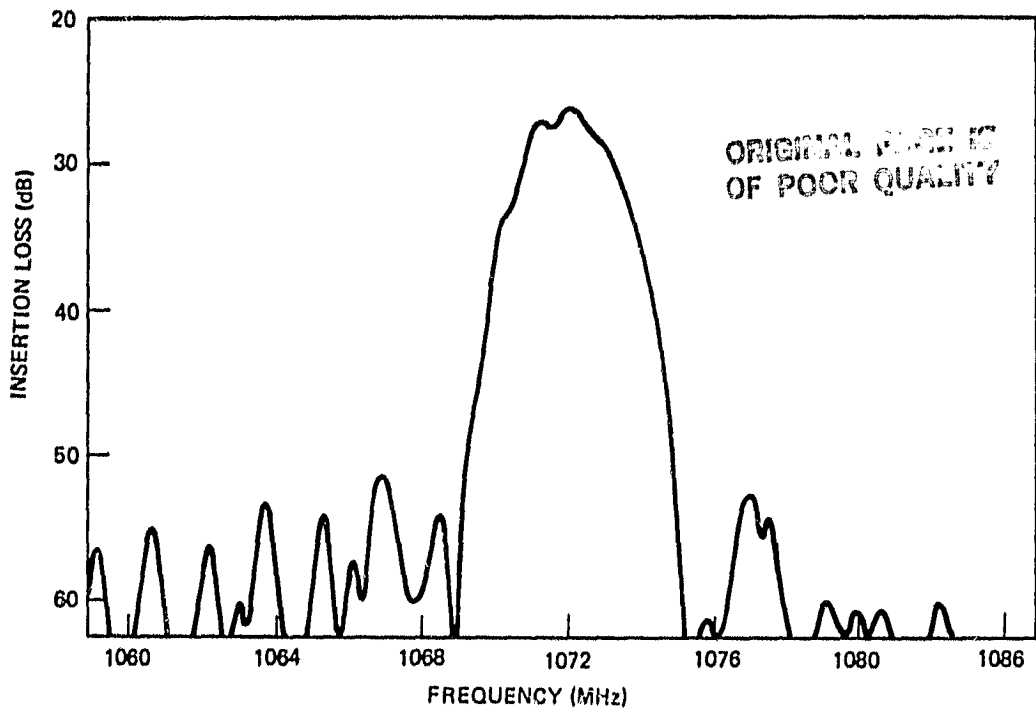


Figure 2-6. Frequency Response of SBAW Delay Line with Third Harmonic Transducers

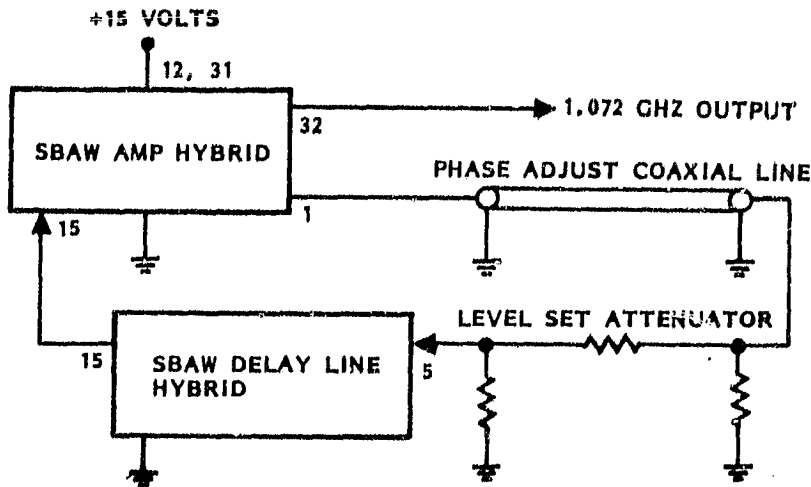


Figure 2-7. 1.072 GHz Hybrid Packaged SBAW Oscillator Schematic

The SBAW oscillator's circuitry was divided into two functional sections which were packaged separately. One hybrid package contained the SBAW delay line. The second contained the 1 GHz amplifier circuitry. A phase set coaxial line and level set attenuator which were used to control the oscillator's feedback characteristics are mounted external to the hybrid packages. The two hybrid packages with a minimum of external circuitry form a complete 1.072 GHz SBAW oscillator. The complete 1.072 GHz SBAW oscillator assembly is mounted on a 3.4 x 2.7 x 0.25 inch brass plate.

The key performance parameters of the four 1.072 GHz SBAW hybrid packaged oscillators are summarized in Table 2-2. The temperature stability of the four 1.072 GHz SBAW oscillators varied from  $\pm 0.0025$  to  $\pm 0.0047\%$  over a  $-20$  to  $+50^\circ\text{C}$  temperature range.

Table 2-2. 1.072 GHz Hybrid Packged SBAW Oscillator Data Summary

Parameter	SN35290	SN35288	SN35296	SN35289
Power Output	+6.6 dBm	+5.5 dBm	+5.5 dBm	+6.1 dBm
Frequency	1.07145 GHz	1.07172 GHz	1.07206 GHz	1.07166 GHz
Frequency Settability	$\pm 0.83$ MHz	$\pm 1.065$ MHz	$\pm 1.035$ MHz	$\pm 0.8$ MHz
Temperature Stability -20 to 50°C	$\pm 0.0033$ %	$\pm 0.0025$ %	$\pm 0.0047$ %	$\pm 0.0042$ %
Phase Noise dBc/Hz				
1 kHz	-86	-84	-84	-84
10 kHz	-106	-105	-105	-105
100 kHz	-126	-126	-125	-125
1 MHz	-145	-144	-142	-140

Aging measurements were also performed on 4 of the 5 oscillators. By the end of Phase I, approximately three months of aging data were collected.

### 2.3 Other Developments

The remaining tasks of the Phase I effort included the investigation of SBAW in  $\text{AlN}/\text{Al}_2\text{O}_3$ , the 2.144 GHz SBAW delay line study, and the frequency selectability and settability study.

Theoretical calculation of wave properties in  $\text{AlN}/\text{Al}_2\text{O}_3$  shows that no coupling exists for a horizontal shear wave bulk mode on basal plane sapphire. As a consequence, it is unlikely to find useful SBAW's

in that material. The 144 SBAW delay line design study pointed to the use of 3rd and 5th harmonic transducers. The investigation of frequency selectability and settability suggests that up to  $\pm 21\%$  change in operating frequency can be achieved with one photomask using substrates of different crystal orientations.

### 3. AGING STUDY OF 1 GHz SBAW OSCILLATORS

The first task of the Phase II program is a continuation of the aging measurement of the 1.072 GHz SBAW oscillators. Four oscillators were aged under continuously operating conditions. The oscillators were mounted on a common baseplate to minimize temperature differentials between units. Before initiation of the aging test, the oscillators were temperature cycled between 10° and 150° F to minimize any frequency hysteresis caused by thermally induced mechanical stress and movement in the oscillator component. The measurements of oscillator frequency, output power and baseplate temperature were performed daily. Temperature of the baseplate is normally 28 ±1°C.

The aging measurement was interrupted several times during the course of the aging study. Each interruption caused a discontinuity in frequency, as shown in Figure 3-1. To properly analyze the data, these discontinuities were removed. Figures 3-2 through 3-5 show the results of the aging measurement. There are 5 ppm of medium term fluctuations over a time period of weeks. Long term baseline drift, on the other hand, is quite small. Table 3.1 summarizes the measured aging rates. These rates are a result of fitting the data to a straight line. Extremely small long term aging rates (< 1 ppm/year) were observed for two of the four oscillators.

Table 3.1 Measured Aging Rates

<u>OSCILLATOR NO.</u>	<u>RATE (PPM/YEAR)</u>	<u>DURATION (MONTH)</u>
35288	-0.47	18
35289	-4.6	16
35290	+2.9	18
35292	-0.1	18

ORIGINAL PAGE IS  
OF POOR QUALITY

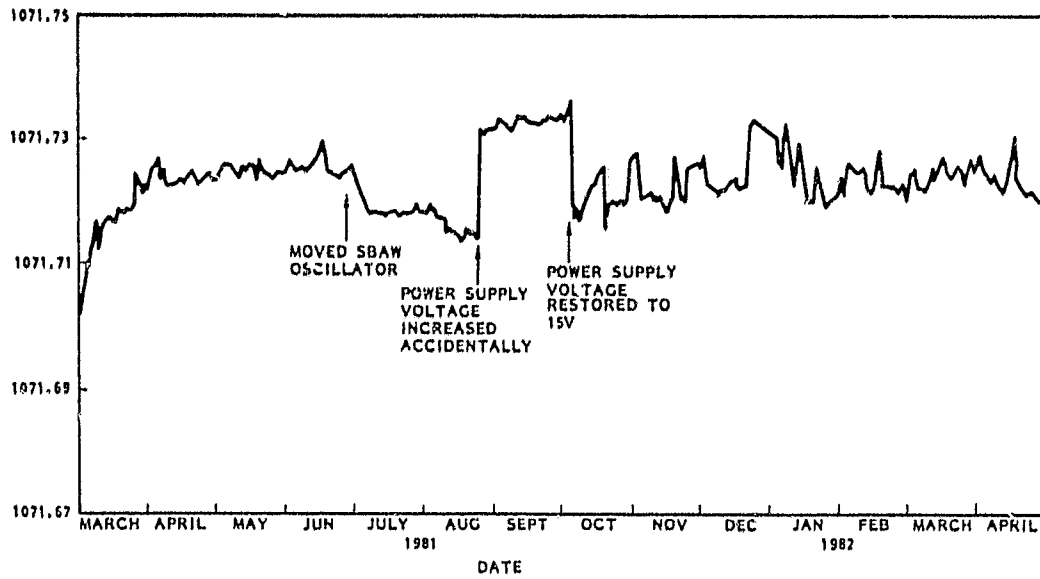


Figure 3.1. Original Data of SBAW Oscillator Number 35288

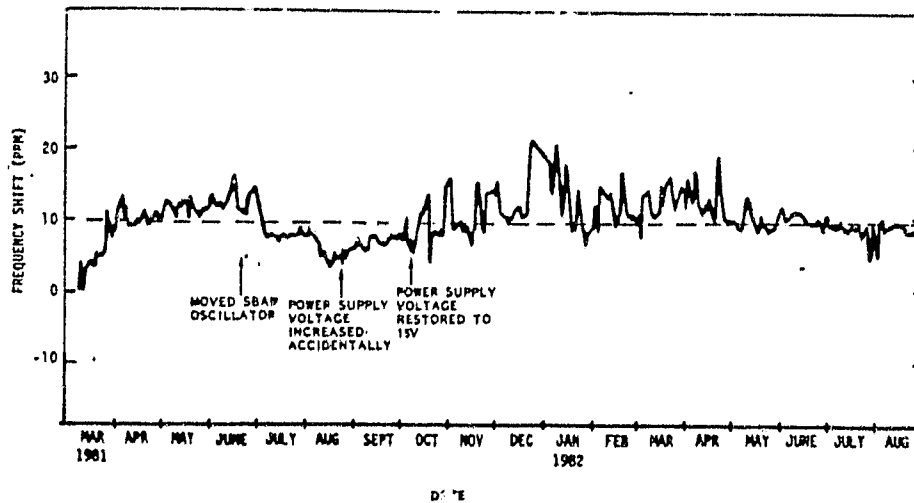


Figure 3.2. Data of SBAW Oscillator Number 35288  
with Discontinuities Removed

ORIGINAL PAGE IS  
OF POOR QUALITY

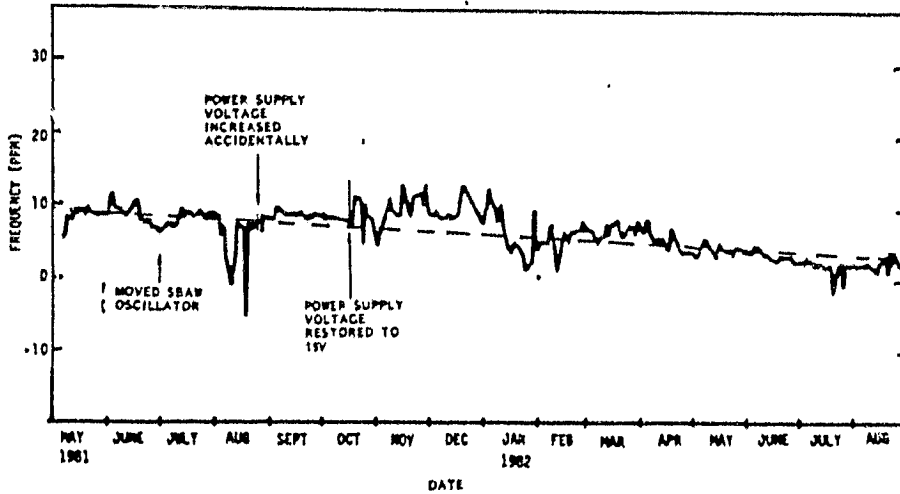


Figure 3.3. Data of SBAW Oscillator Number 35289 with Discontinuities Removed

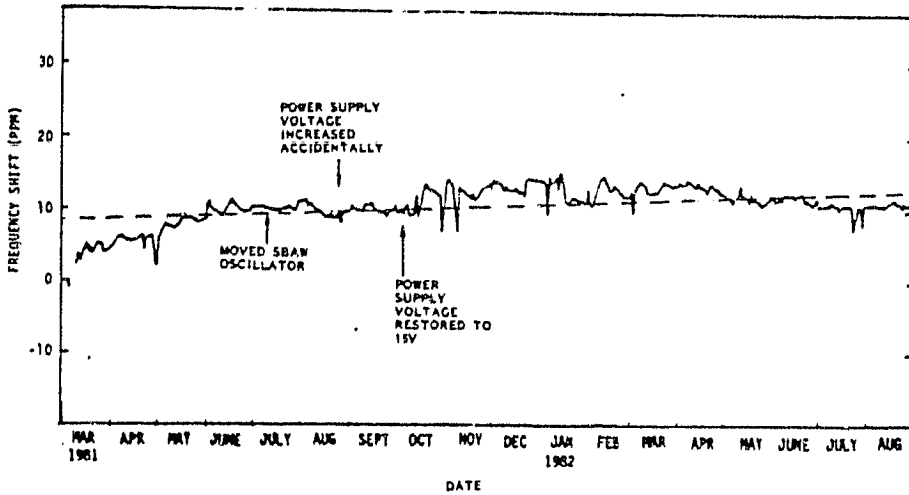


Figure 3.4. Data of SBAW Oscillator Number 35290 with Discontinuities Removed

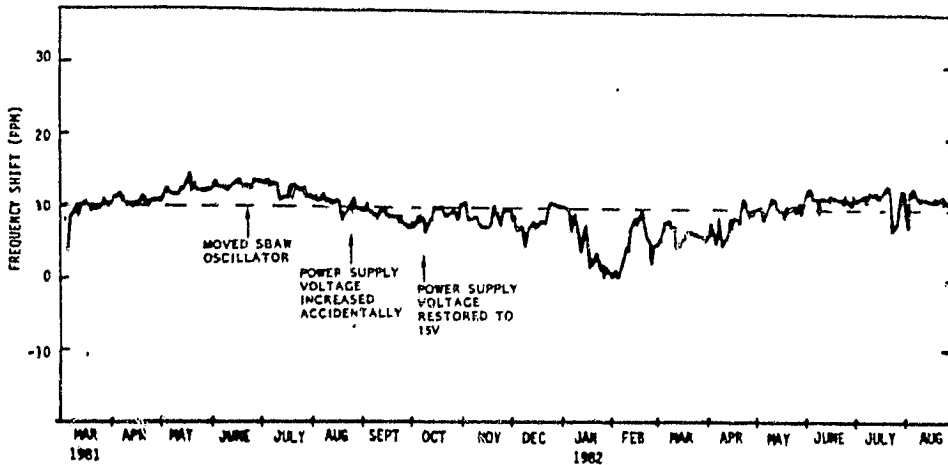


Figure 3.5. Data of SBAW Oscillator Number 35292 with Discontinuities Removed

#### 4. 2 GHz SBAW DELAY LINE DEVELOPMENT

The development of the 2 GHz SBAW delay line is based on the analysis and experimental results of the Phase I effort which established the harmonic operating transducers as the baseline approach. Since there are two temperature stable cuts found in the singly rotated Y-cut quartz family, both were investigated to determine which one is more suitable for delay line oscillator application.

##### 4.1 Devices on 36.25° Rotated Y Cut Quartz

The 1.072 GHz device developed in Phase I uses 36.25° rotated Y cut quartz as the substrate. The SBAW in this substrate is somewhat less temperature stable than the SAW in ST quartz. A comparison of temperature stabilities of two stable SBAW cuts and the SAW in ST quartz is shown in Figure 4.1. The advantages of the 36.25° rotated Y-cut quartz SBAW over the -50.25° rotated Y cut SBAW are that it has a faster wave velocity, and a higher degree of coupling, resulting in a lower insertion loss. A design based on the 3rd harmonic transducer approach was implemented using this substrate and was found to yield good device performance. The design parameters of the delay line are listed in Table 4.1, and its performance parameters in Table 4.2. The frequency response of this device is shown in Figure 4.2.

Table 4.1. Design of the Third Harmonic SBAW Delay Line

FINGER WIDTH ( $\mu\text{M}$ )	0.8918
TRANSDUCER LENGTH ( $\lambda_0$ )	451
OSCILLATOR Q	1496
3 dB BANDWIDTH (MHz)	2.95
SUBSTRATE	36.25° ROTATED Y-CUT QUARTZ

Table 4.2. Performance of the Third Harmonic SBAW Delay Line

CENTER FREQUENCY	2141.7 $\pm$ 1.0
3 dB BANDWIDTH (MHz)	3.4 $\pm$ 0.3
UNMATCHED INSERTION LOSS (dB)	2.7
OSCILLATOR Q	1441

ORIGINAL PAGE IS  
OF POOR QUALITY

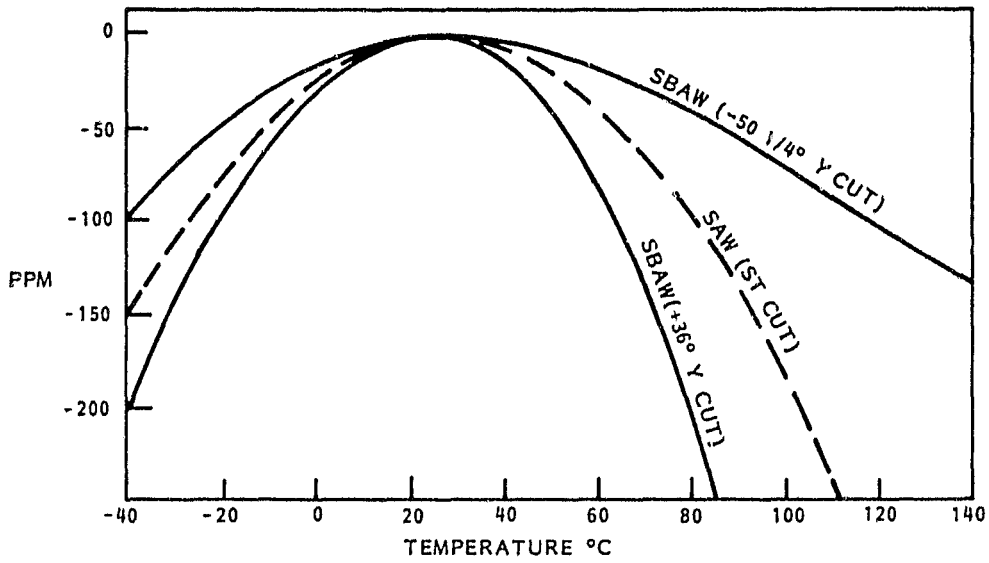


Figure 4.1. Comparison of Temperature Stability Between SAW and SBAW Devices

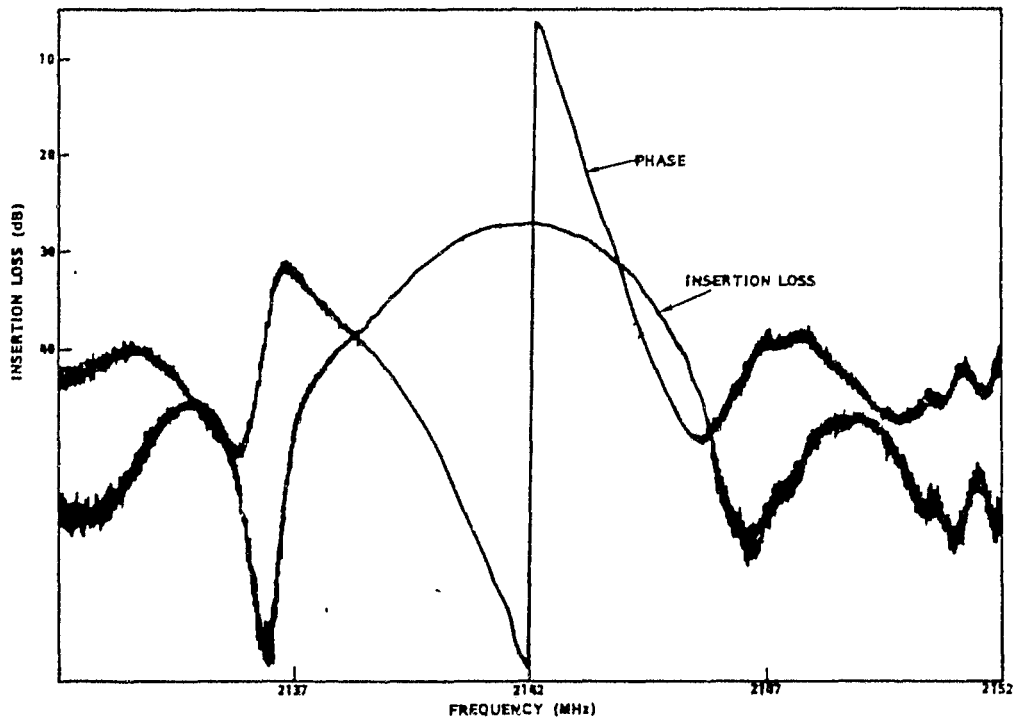


Figure 4.2. Frequency Response of SBAW Device with Third Harmonic Transducers

Prior to the design and fabrication of the device of Figure 4.2, a series of experiments were performed to determine the tradeoff between insertion loss and phase slope (oscillator Q) of the delay line on  $36.25^\circ$  rotated Y-cut quartz. Oscillator Q for the device is defined as  $\omega t/2$ , where  $\omega$  is the oscillator frequency in units of radians, and  $t$  is the delay time. The short term stability of the oscillator, controlled by the SBAW delay line, is such that for maximum stability the SBAW device must have minimum insertion loss and highest Q, or rapidly changing phase slope as a function of frequency. In actual devices, however, high Q means a larger separation between transducers and therefore higher propagation loss.

A device was designed to have a transducer whose length is 750 wavelengths long at the operating frequency. The insertion loss of this device fabricated with  $400 \text{ \AA}$  of aluminum embedded in  $350 \text{ \AA}$  grooves was typically 40 dB. The length of the transducer was then reduced systematically by laser trimming. In this laser trimming experiment, the fingers at the outer edges of the SBAW transducer were disconnected by evaporating the finger metallization with a laser pulse. The length of the transducer was effectively shortened. At each stage of the experiment, the insertion loss of the device was measured. The results of this study showed that for  $36.25^\circ$  rotated Y-cut devices,  $450 \lambda$  represents an optimum transducer length.

#### 4.2 Devices on $-50.5^\circ$ Rotated Y Cut Quartz

The wave velocity of the SBAW in  $-50.5^\circ$  rotated Y cut quartz is much slower than that of the  $36.25^\circ$  cut substrate. To achieve 2.143 GHz using the third harmonic design requires finger widths of  $0.58 \mu\text{m}$ . Such line widths border at the limit of photolithographic techniques. To relieve such stringent fabrication tolerance, a fifth harmonic design was adopted. The fifth harmonic design employs a 6 finger per period, in a 3-up, 3-down configuration, as shown in Figure 4.3. The design details of this device are listed in Table 4.3.

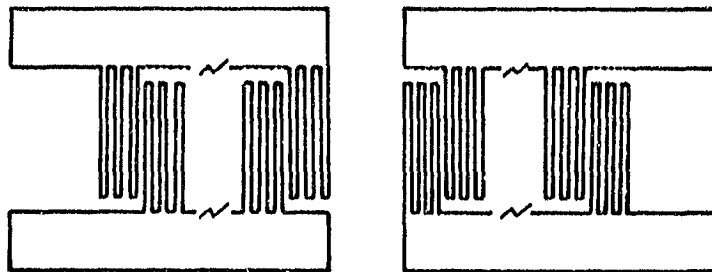


Figure 4.3. Fifth Harmonic 2.144 GHz Delay Line

Table 4.3. Design of the Fifth Harmonic SBAW Delay Line

- FINGER WIDTH =  $0.65 \mu\text{m}$
- TRANSDUCER LENGTH =  $750\lambda_0$
- OSCILLATOR Q = 2479
- 3 dB BANDWIDTH = 1.9 MHz
- $-50.5^\circ$  ROTATED Y CUT QUARTZ

Performance of the device on  $-50.5^\circ$  rotated Y cut quartz varied from device to device. Their unmatched insertion loss is at the order of 35-45 dB. One of the lowest loss devices shown in Figure 4.4 was matched to show only 24 dB of insertion loss. The temperature stability of the device was measured by incorporating the delay line into an oscillator loop. The data from the temperature measurement is shown in Figure 4.5.

The SBAW devices on  $-50.5^\circ$  rotated Y cut quartz exhibit two features which are not obvious from theoretical predictions. The insertion loss of the device was found to be affected very little by embedding the transducer fingers as long as the metallization was kept thin. The device reported in Figure 4-4, for example, was fabricated without

ORIGINAL PAGE IS  
OF POOR QUALITY

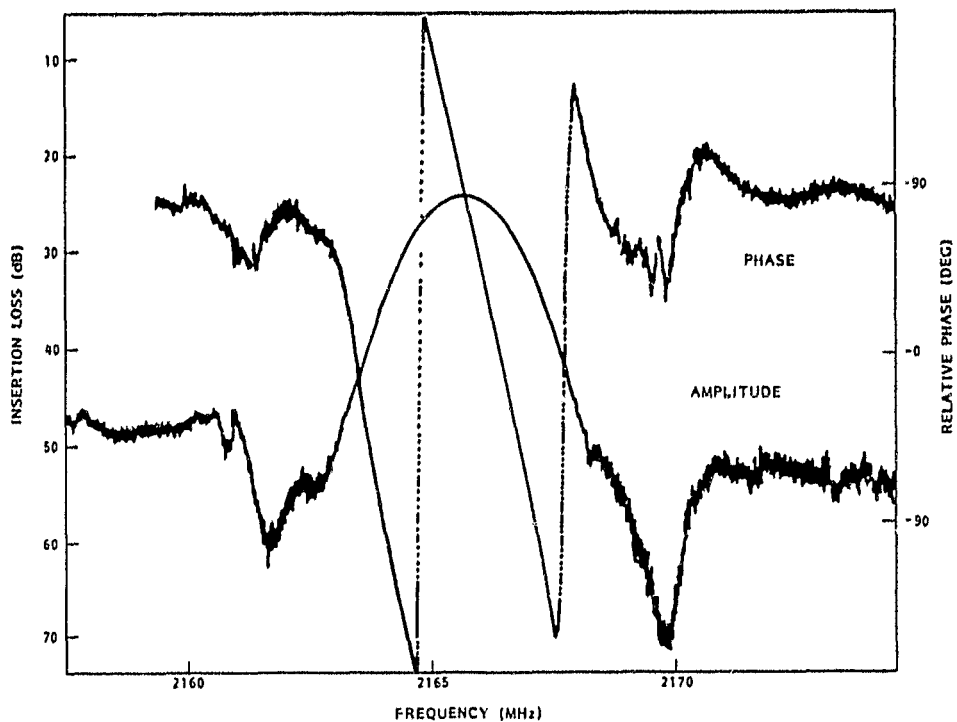


Figure 4.4. Amplitude and Phase Response of a Matched Fifth Harmonic Device on  $-50.5^\circ$  Rotated Y-Cut Quartz

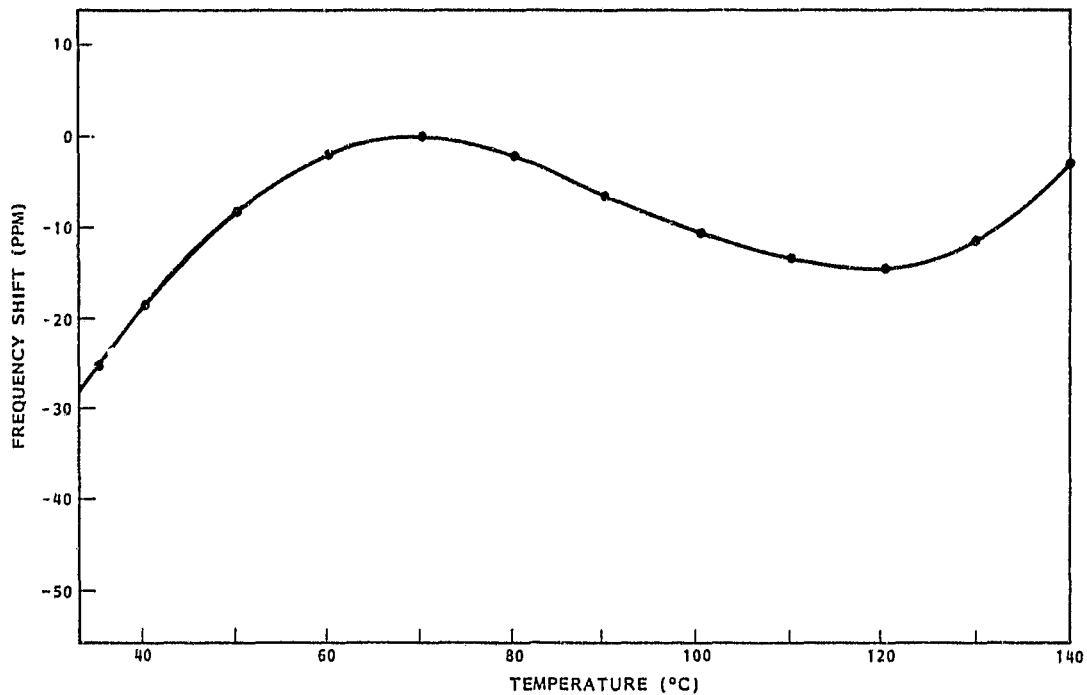


Figure 4.5. Temperature Stability of 2.144 GHz SBAW Delay Line on  $-50.5^\circ$  Rotated Y-Cut Quartz

embedded transducers by using  $350 \text{ \AA}$  of aluminum. A five dB difference in insertion loss would normally be expected from a third harmonic  $35.5^\circ$  rotated Y cut device if the fingers were not embedded. The second feature of the  $50.5^\circ$  rotated Y cut SBAW device is that the optimum length of the transducer is much longer than that of the  $35.5^\circ$  device. Laser trimming experiments performed on the device with a transducer length of  $750 \lambda$  indicate that the optimum length is larger than  $750 \lambda$ . It therefore seems that while the wave velocity and coupling coefficient are lower than the  $35.5^\circ$  device, the  $-50.5^\circ$  rotated Y-cut substrate exhibited the combined properties of high Q ( $> 3000$ ) and good temperature stability at the frequency range near 2 GHz.

#### 4.3 Fabrication and Packaging Techniques

Two fabrication techniques were employed for the device fabrication, depending on whether the transducer fingers were embedded. For the unembedded transducer, the etching technique was used. As shown in Figure 4.6, a thin metal film is deposited on the quartz substrate

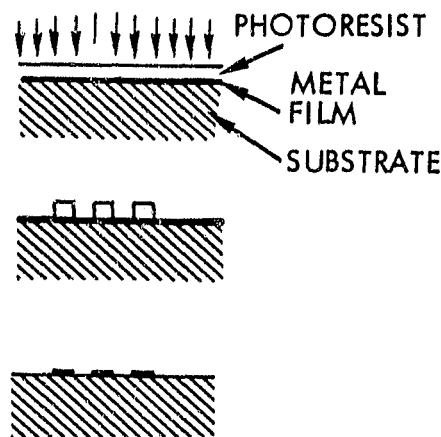


Figure 4-6. Schematic Illustration of Etching Technique

followed by spin coating of Shipley 1350J positive photoresist. The resist is then exposed with a highly uniform monochromatic UV light source through a light field photomask. After exposure, the resist is developed, forming a transducer pattern over the metal film. The metallic pattern is defined by ion beam etching through the developed photoresist pattern. Ion beam etching was found to produce lines with better definition and reproducibility than the conventional chemical etching.

The fabrication process for the embedded transducer is shown schematically in Figure 4.7. After the photoresist pattern is developed, the substrate is ion-milled to create the desired groove depth. Aluminum metallization is then evaporated to fill up the grooves and the resist removed using acetone as the final step. The metal thickness must be within  $100 \text{ \AA}$  of the groove depth. This can be verified by a surface profile measurement using a Dektak machine. A titanium layer of  $30\text{-}40 \text{ \AA}$  can also be placed between the substrate and the aluminum to improve film adhesion.

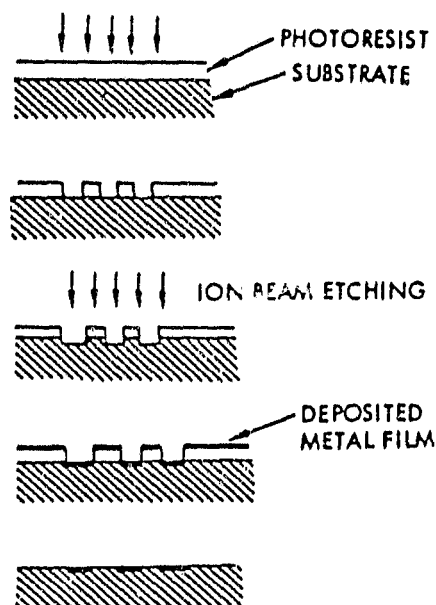


Figure 4-7. SBAW Delay Line Fabrication  
(Embedded Transducer)

The SBAW delay line was packaged in a 20-pin Tekform flatpack. The procedures for device packaging are described below.

The SBAW delay line was mounted in the flatpack with a 71-1 Ablestik adhesive. Only a small drop of Ablestik was applied to the back of the delay line so that most of the SBAW substrate is free from any stress that may arise from mounting. The Ablestik was cured in an oven with a continuous hydrogen flow for one hour at  $300^{\circ}\text{C}$ . Ablestik was selected because of its low outgassing rate, thereby increasing the possibility of having low aging rates.

#### 4.4 Electromagnetic Feedthrough

The electrical performances of the SBAW devices described in Sections 4.1 and 4.2 were measured using a test fixture with greater than 60 dB feedthrough suppression designed specifically for the testing of unpackaged devices. After the device is packaged in the 20 pin flatpack, the device performance deteriorates due to electromagnetic feedthrough. The main effect of the feedthrough is reduced sidelobe level. When the feedthrough level is comparable to the signal, distortion in passband shape can also result. Since the feedthrough level of the flatpack is at the order of -40 dB at 2 GHz, the performance of the  $-50.5^\circ$  rotated Y cut device is degraded to the extent that it is not usable in the oscillator circuit. Due to time and equipment constraints, further research into different packages was not feasible. Only the devices fabricated on  $36.25^\circ$  rotated Y cut quartz were used for oscillator application.

## 5. 2 GHz SBAW OSCILLATOR DEVELOPMENT

### 5.1 Detail Design

The 2 GHz SBAW oscillator is mounted on a 3" x 3 1/2" brass baseplate as shown in Figure 5-1.

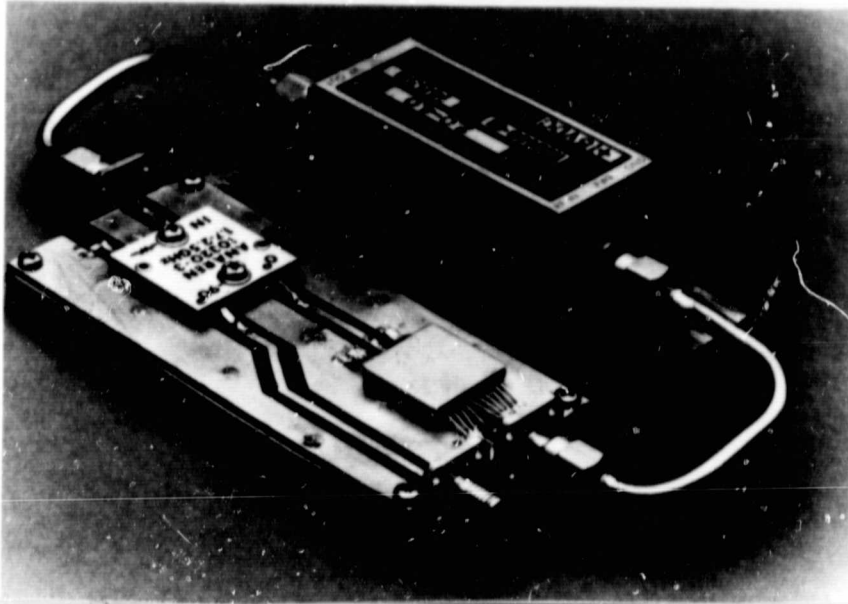


Figure 5.1. 2 GHz SBAW Oscillator

The schematic diagram is shown in Figure 5-2, and the drawing is shown in Figure 5-3.

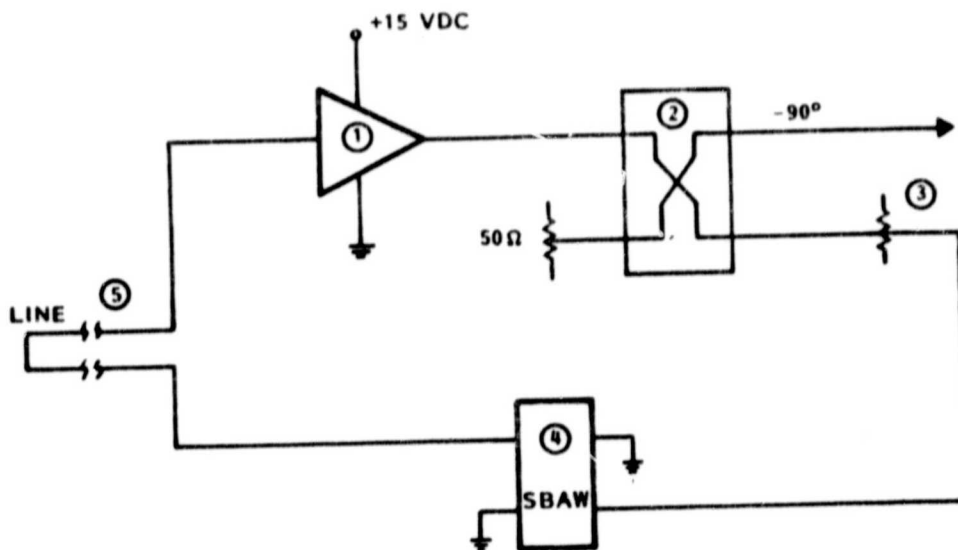


Figure 5-2. 2.144 GHz Oscillator Block Diagram

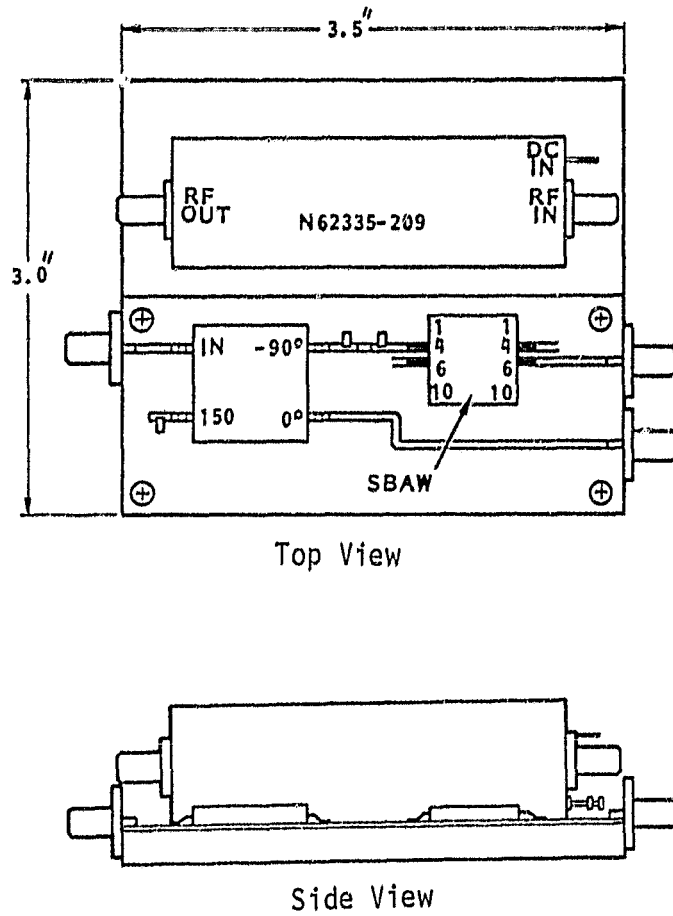


Figure 5-3. Drawings of the 2 GHz SBAW Oscillator

The components used in the oscillator circuit and their gain/loss analysis are listed in Table 5.1.

Table 5.1. Component/Gain of Oscillator Loop.

<u>COMPONENT</u>	<u>GAIN/LOSS (dB)</u>
1 (a) NARDA N-62335-211 Amplifier	+33.00
1 (b) NARADA N-6233S-209 Amplifier	+44.00
2 Anaren 10230-3 Quadrature Hybrid	- 3.25
3 Resistive Pad	TBD
4 SBAW Device	-26.00
5 Variable Length Line	- 0.10
Excess Loop Gain	4.0-6.0

The quadrature hybrid power splitter and the SBAW device were assembled on a 25 mil thick Duroid circuit board which was mounted on the base plate. The loop amplifier, on the other hand, was mounted directly to the baseplate. Out of the 5 amplifiers there were three that had 33 dB gain and two that had 44 dB gain. The resistive pad was used to adjust the excess loop gain to within 4 to 6 dB. Semi-rigid coaxial cables were used to connect the amplifier to the circuit board. Frequency adjustment was accomplished by varying the length of these cables.

## 5.2 Spurious Output and Phase Noise Characteristics

Five oscillators were constructed, one of which has the SBAW delay line mounted in a flatpack without its cover for display purposes. Performance data was taken on the remaining four oscillators and is summarized in Table 5-2.

A typical spectrum analyzer measured output of a SBAW oscillator is shown in Figure 5.4. No spurious noise is observed at frequencies close to the desired output frequency. The output power is +18.3 dBm for this oscillator. When a much wider frequency range is searched, harmonics of the fundamental frequency are observed up to 15 GHz (Figure 5.5). These harmonics are due to the nonlinear characteristics of the loop amplifier when it is driven into saturation and is typical of this type of oscillator.

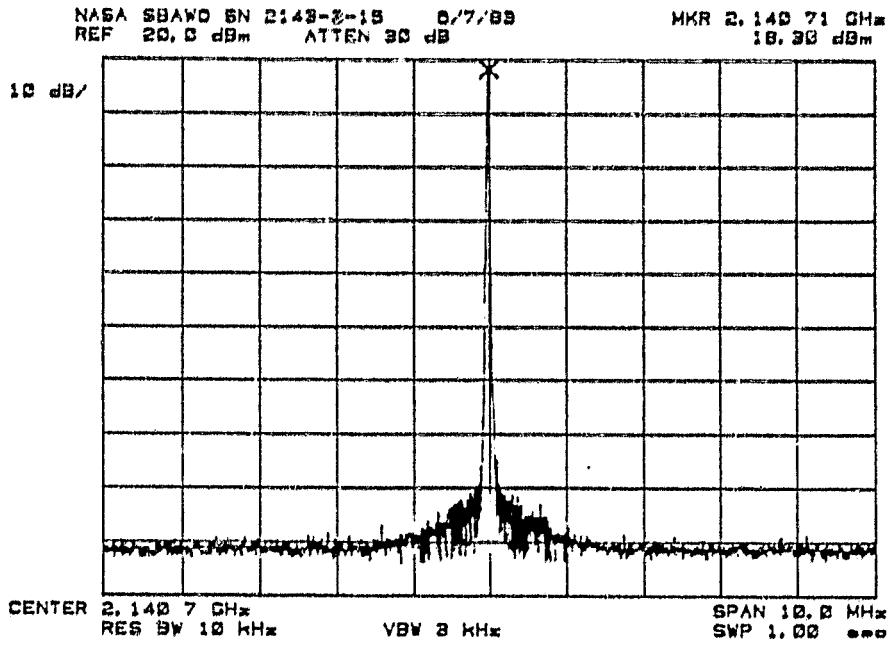


Figure 5-4. Spectrum Analyzer Measurement of Oscillator Output

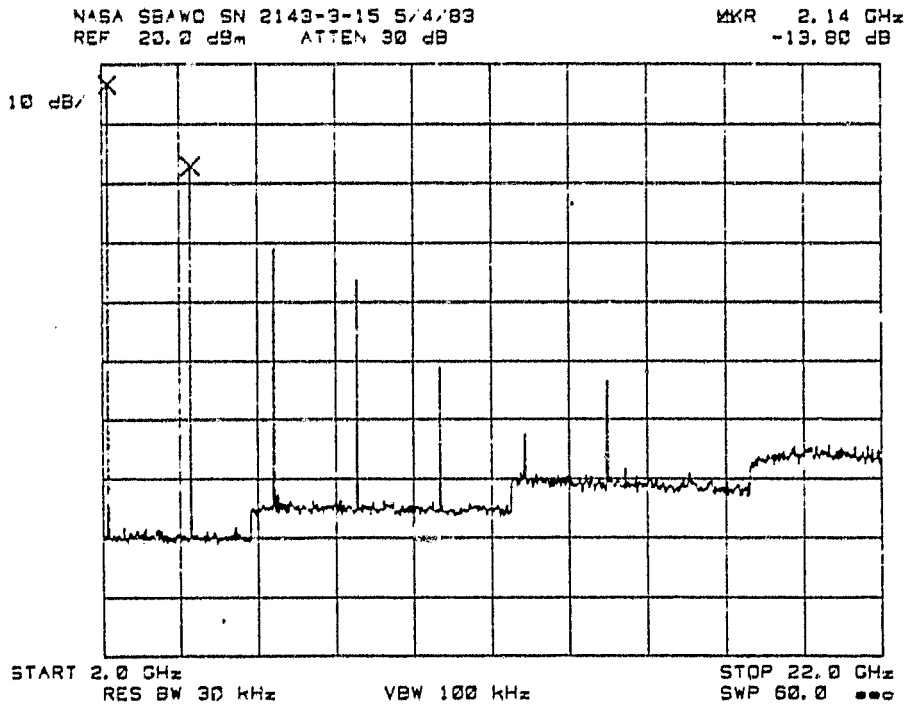


Figure 5.5. Harmonic Frequencies of the Oscillator

Table 5-2. 2.14 GHz SBAW Oscillator Data Summary

PARAMETER	2143-3-07	2143-3-08	2143-3-11	2143-3-15
OUTPUT FREQUENCY GHz	2.143282	2.143590	2.143862	2.140749
OUTPUT POWER, dBm	+14.5	+13.1	+15.5	+18.0
TEMPERATURE STABILITY, ppm (-20 to +50°C)	±42	±30	±48	±22
SSB PHASE NOISE, dBc/Hz at				
1 KHz	-70	-70	-68	-64
10 KHz	-100	-103	-98	-94
100 KHz	-132	-133	-126	-126
1 MHz	-158	-158	-156	-155

The phase noise characteristics of the oscillators are shown in Figures 5-6 through 5-9. They were measured in the TRW Metrology Department using computer controlled phase noise measurement equipment. This fully automated system is based on the HP3585A, 8566A, and 8568A analog type automatic spectrum analyzers and the HP5420A digital signal analyzer (dual-channel fast Fourier transform type). The controller is the HP9845T desktop computer. The system provides the basic capability of measuring phase noise from microhertz to the 1500 MHz Fourier frequency range of the carrier.

A plot of the theoretical calculation of the phase noise characteristics based on amplifier noise figure, device insertion loss, loop power and device delay time is shown as the dotted line in Figure 5-6. The agreement between theory and experiment is good. The  $1/f^3$  dependence of the phase noise indicated that the dominant noise process in the oscillator is flicker FM.

ORIGINAL PAGE IS  
OF POOR QUALITY

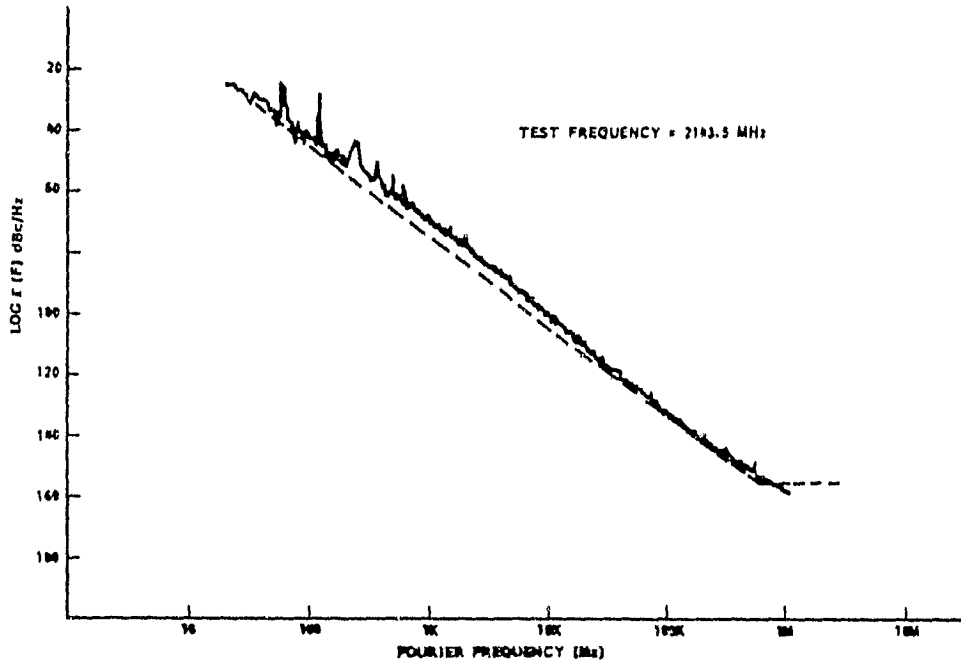


Figure 5.6. Normalized Phase Noise Sideband Power Spectral Density for Oscillator SN 2143-3-07

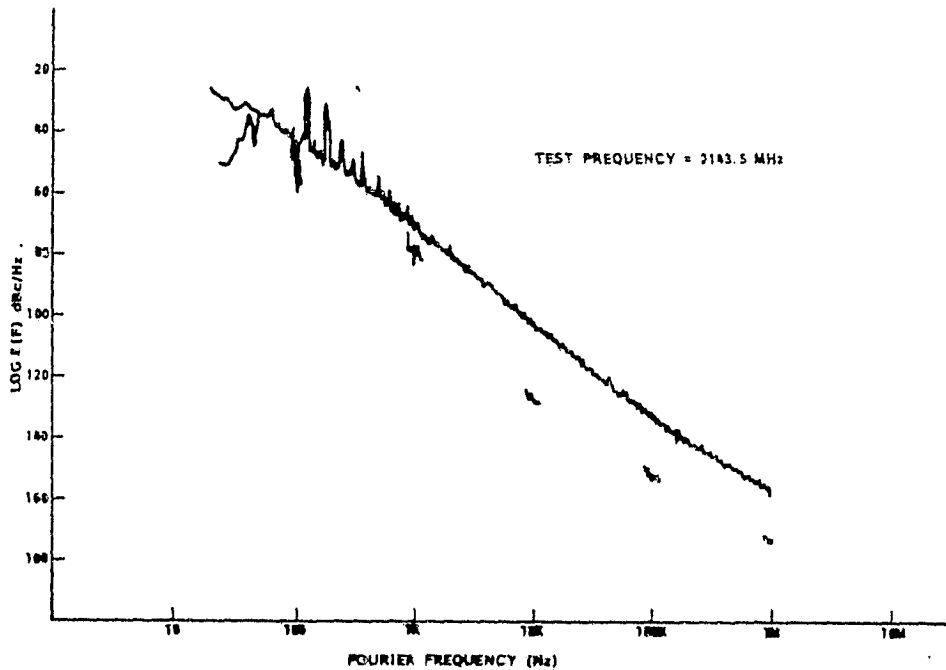


Figure 5-7. Normalized Phase Noise Sideband Power Spectral Density for Oscillator SN 2143-3-08.

ORIGINAL PAGE IS  
OF POOR QUALITY

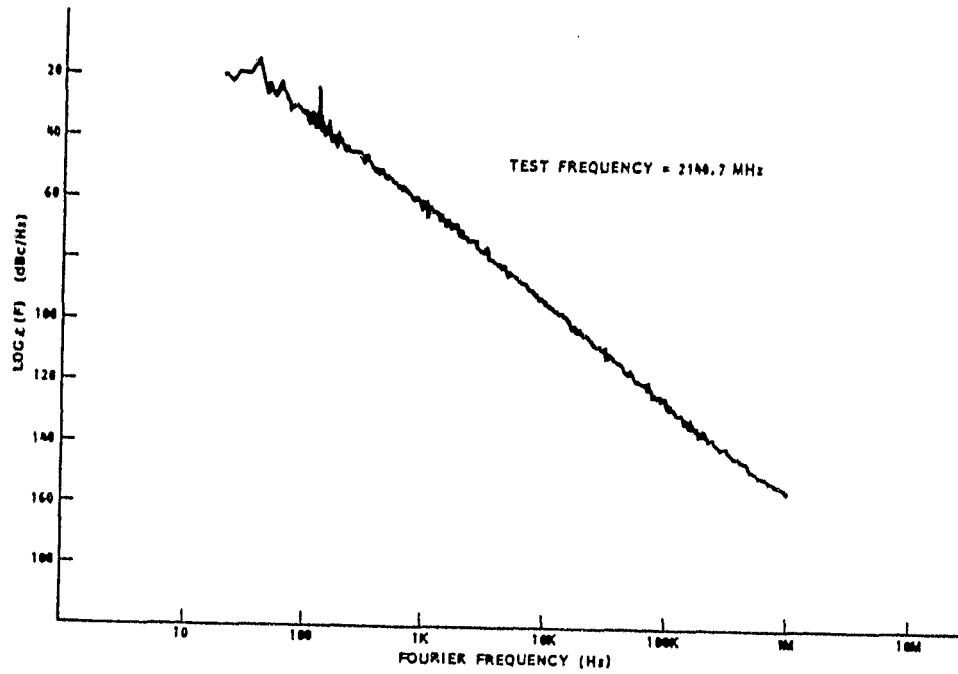


Figure 5-8. Normalized Phase Noise Sideband Power Spectral Density for Oscillator SN 2143-3-11

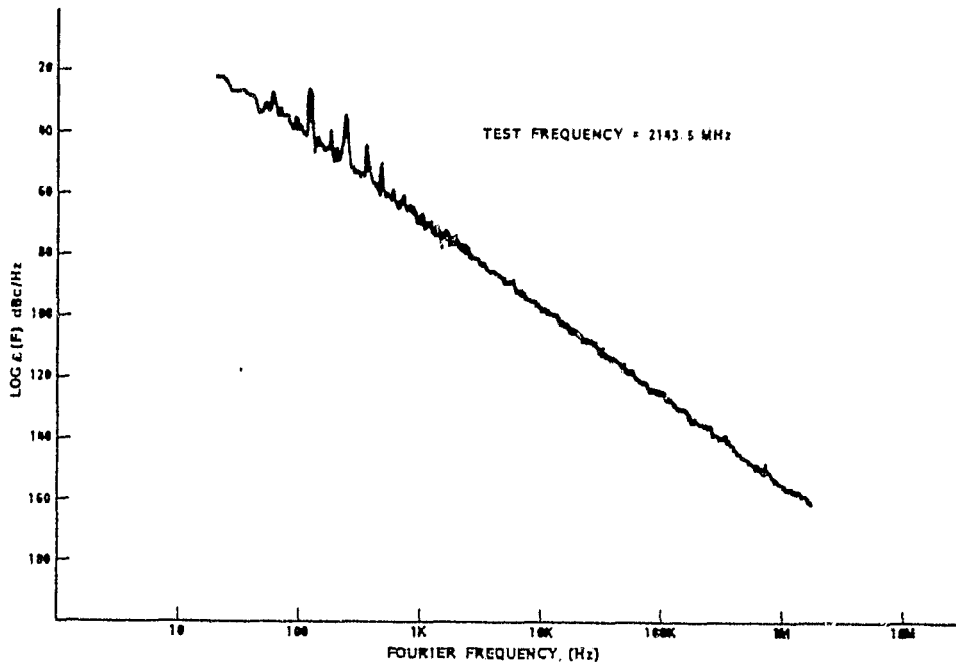


Figure 5-9. Normalized Phase Noise Sideband Power Spectral Density for Oscillator SN 2143-3-15

### 5.3 Temperature Stability

The temperature stability of the SBAW oscillator was measured using an experimental set-up which automatically cycles the temperature of the environmental chamber and records the output frequency of the oscillator. During each experiment one oscillator was placed inside the chamber, and the temperature of the chamber was cycled up and down in  $10^{\circ}$  C steps over the range between  $-20^{\circ}$  C and  $60^{\circ}$  C. At least 15 minutes was allowed at each temperature step before the frequency measurement was taken so that the device had time to reach thermal equilibrium within the chamber.

The results of the temperature stability measurements are shown in Figs. 5-10 through 5-13. The turnover temperature generally lies between  $10^{\circ}$  and  $20^{\circ}$  C. Absolute frequency excursion between  $-20^{\circ}$  C to  $50^{\circ}$  C varied from  $\pm 22$  ppm to  $\pm 48$  ppm. The parabolic temperature dependence is typical of devices fabricated on  $36.25^{\circ}$  rotated Y cut quartz.

### 5.4 Long Term Aging Characteristics

The long term stability of the SBAW oscillator is determined by the long term stability of the SBAW delay line. The aging characteristics of the SBAW delay line are thought to depend on many complex factors, including crystal polish, metal film stress, device mounting stress, contamination and device packages. Since good aging was observed for the 1 GHz SBAW delay lines, similar mounting and packaging techniques were employed for the 2 GHz device. The SBAW delay lines were attached to the 20-pin Tekform flatpack using 71-1 Ablestik adhesive. Only a small drop of Ablestik was used at the center portion of the crystal, therefore allowing most of the substrate to be free from any stress. The Ablestik was cured in an oven with continuous hydrogen flow for one hour at  $300^{\circ}$  C. The devices were then hermetically sealed with resistive welding in a nitrogen atmosphere.

Aging of three SBAW oscillators began on December 13, 1982. The oscillators were mounted onto a common aluminum baseplate. A thermocouple was attached to the baseplate so that the temperature could be monitored. Over the duration of the aging experiment, the baseplate temperature variation was  $\pm 1^{\circ}$  C. Figures 5-14 through 5-16 show the variations in output frequency as a function of time. A discontinuity

TEMPERATURE STABILITY  
OF OSCILLATOR

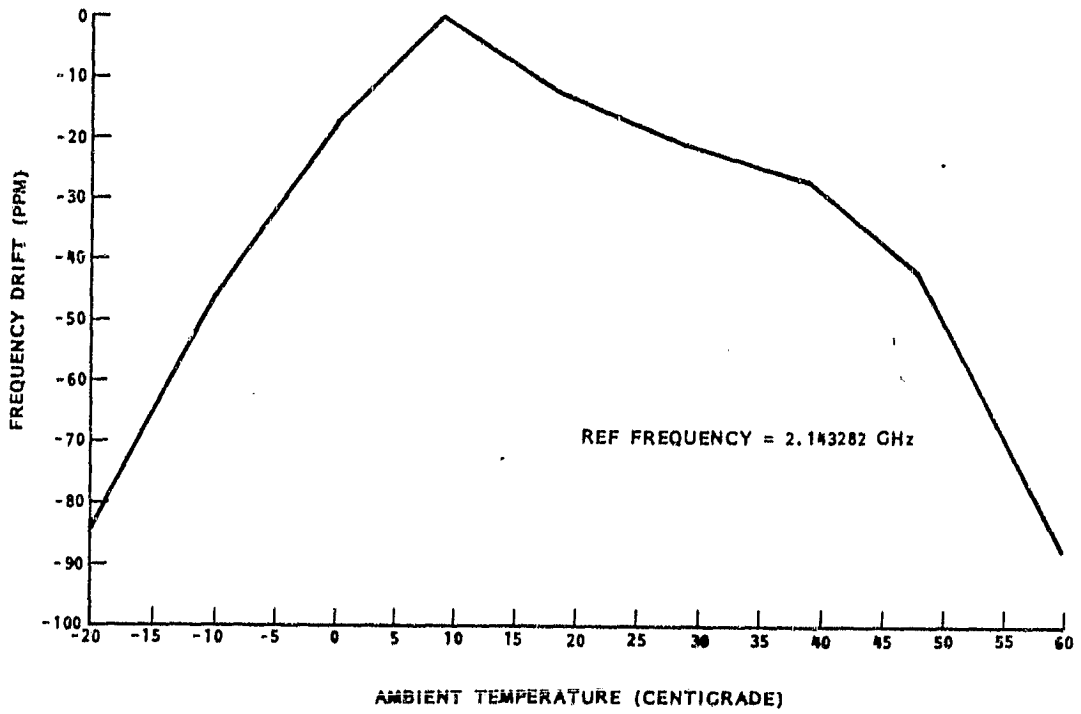


Figure 5-10. Temperature Stability of Oscillator SN 2143-3-07

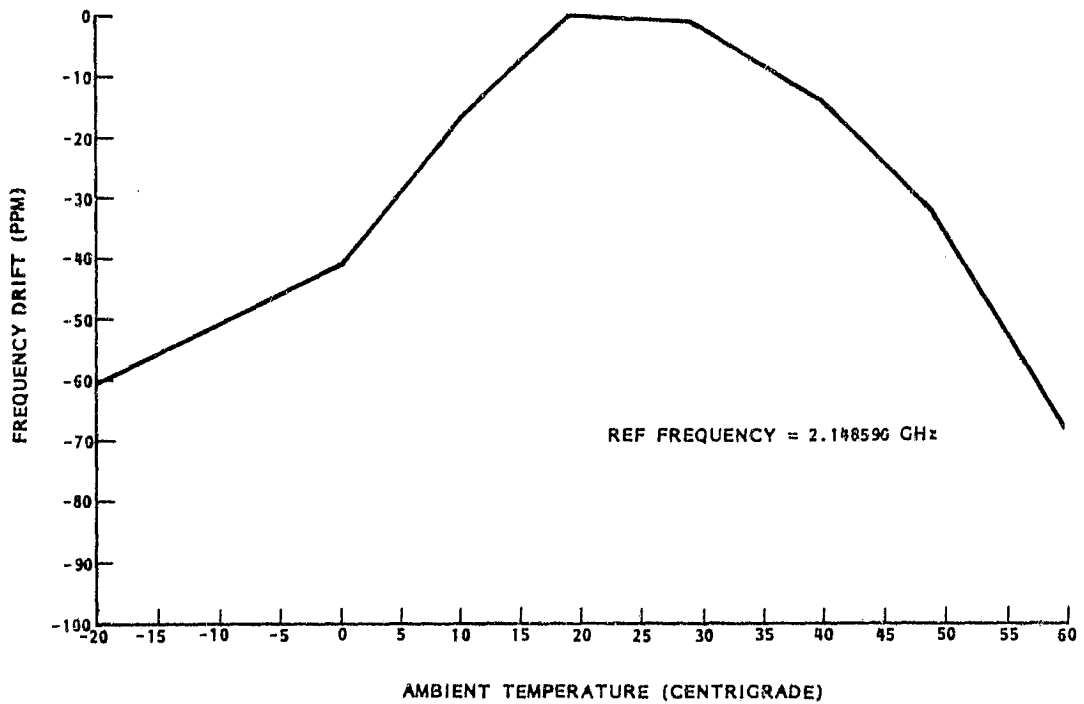


Figure 5-11. Temperature Stability of Oscillator SN 2143-3-08.

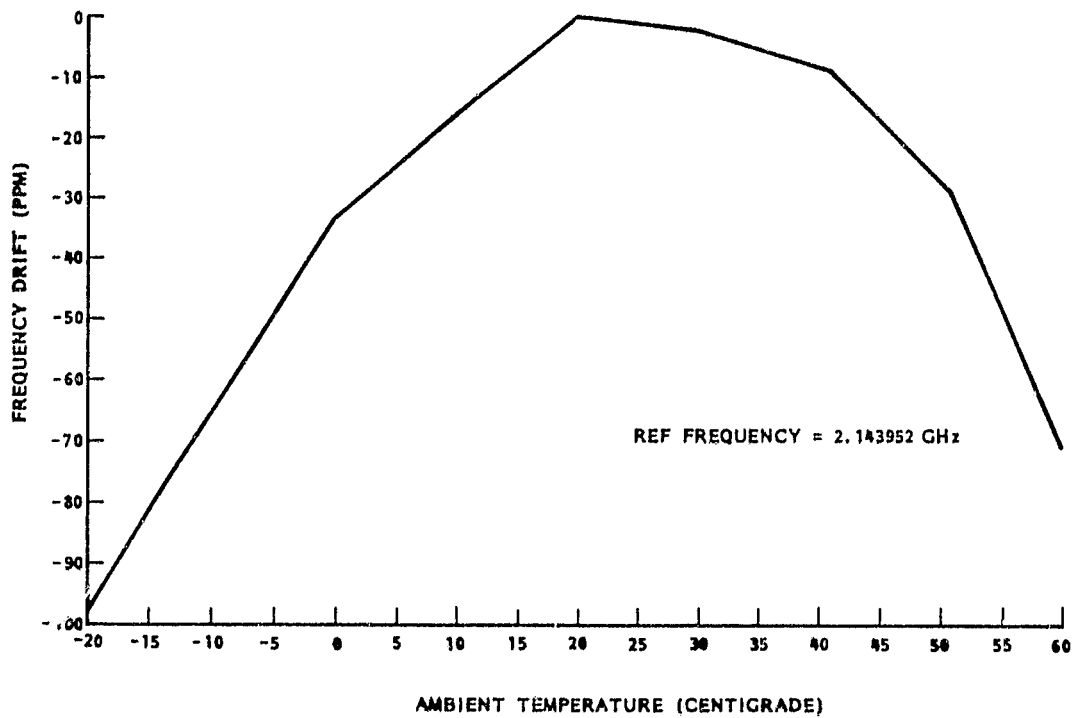


Figure 5-12. Temperature Stability of Oscillator SN 2143-3-11.

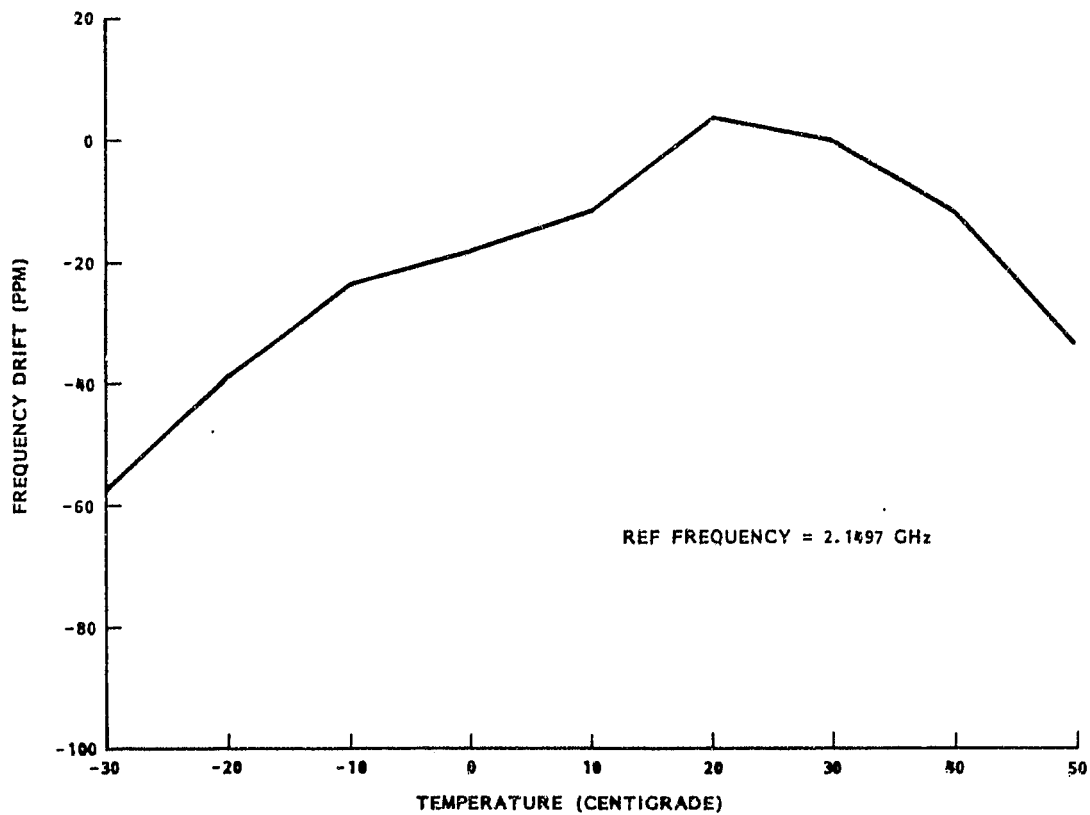


Figure 5-13. Temperature Stability of Oscillator SN 2143-3-15.

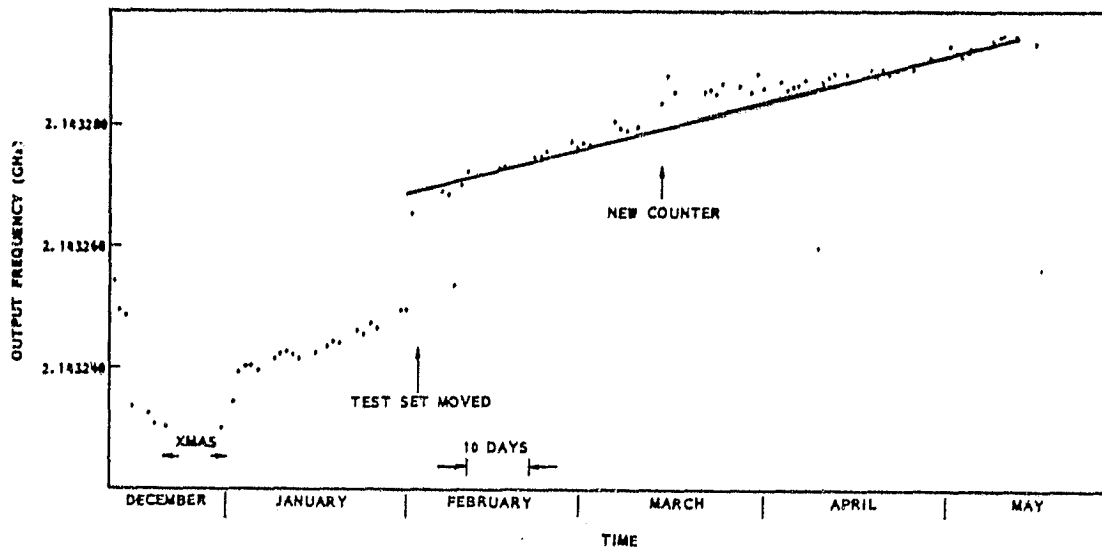


Figure 5-14. Long Term Stability of Oscillator SN 2143-3-07.

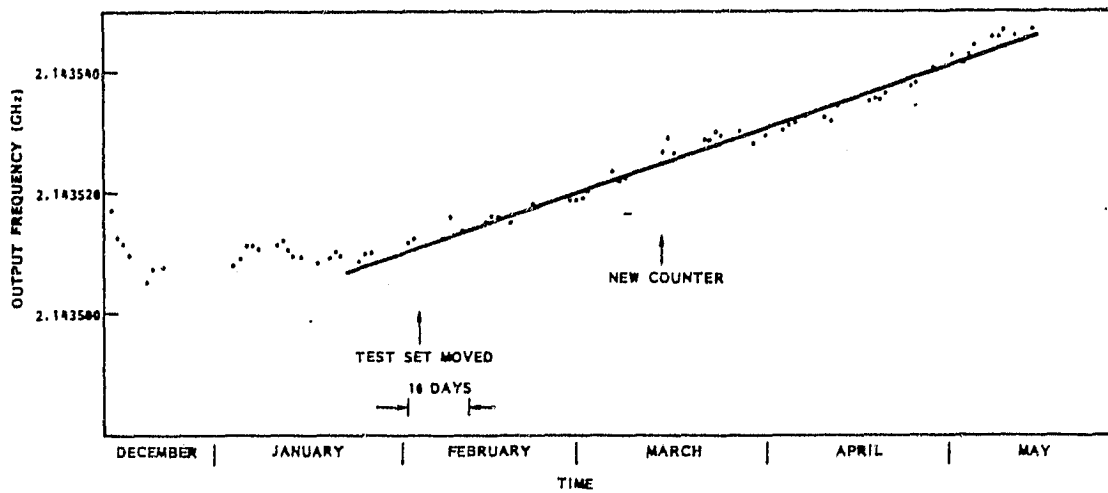


Figure 5-15. Long Term Stability of Oscillator SN 2143-3-08.

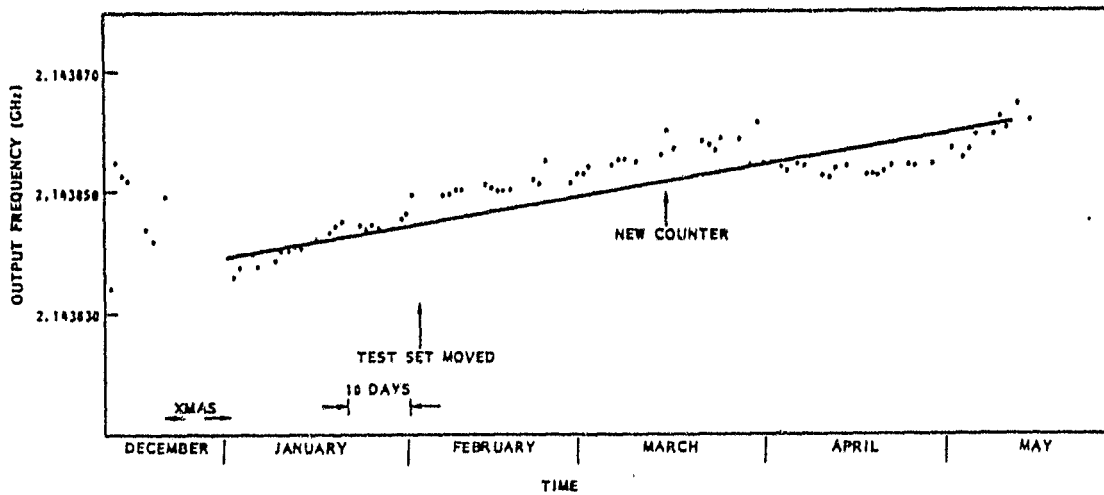


Figure 5-16. Long Term Stability of Oscillator SN 2143-3-11.

appears in one of the plots, this occurred on the day the test set was moved to a new laboratory.

Table 5.3 summarizes the estimated aging rates of the oscillators as determined by a least-squares straight line fit to the measured data. This much higher aging rate compared to the 1 GHz SBAW oscillator's was disappointing. Therefore, it was decided that meaningful data could be obtained by temperature cycling all three oscillators between  $-12^{\circ}\text{C}$  and  $54^{\circ}\text{C}$  and then continuing the aging measurement for an additional three months. A fourth oscillator (SN 2143-3-15) was also temperature cycled and added to increase the data base. The results of the additional measurements are summarized in Figure 5-17. The oscillator SN 2143-3-11 showed random frequency fluctuations. The SN 2143-3-08 unit continued its upward frequency drift, although its rate was reduced to 37.5 ppm/year from 59.4 ppm/year. The SN 2143-3-07 unit showed less than 1 ppm/year aging rate, and SN 2143-3-15 had a  $-10.4$  ppm/year rate.

Table 5.3 NASA 2 GHz SBAW Oscillator Aging Rates

SER. NO.	AGING RATE (ppm/year)	TEST INTERVAL (days)
2143-3-07	+42.6	100
2143-3-08	+59.4	115
2143-3-11	+28.8	130

ORIGINAL PAGE IS  
OF POOR QUALITY

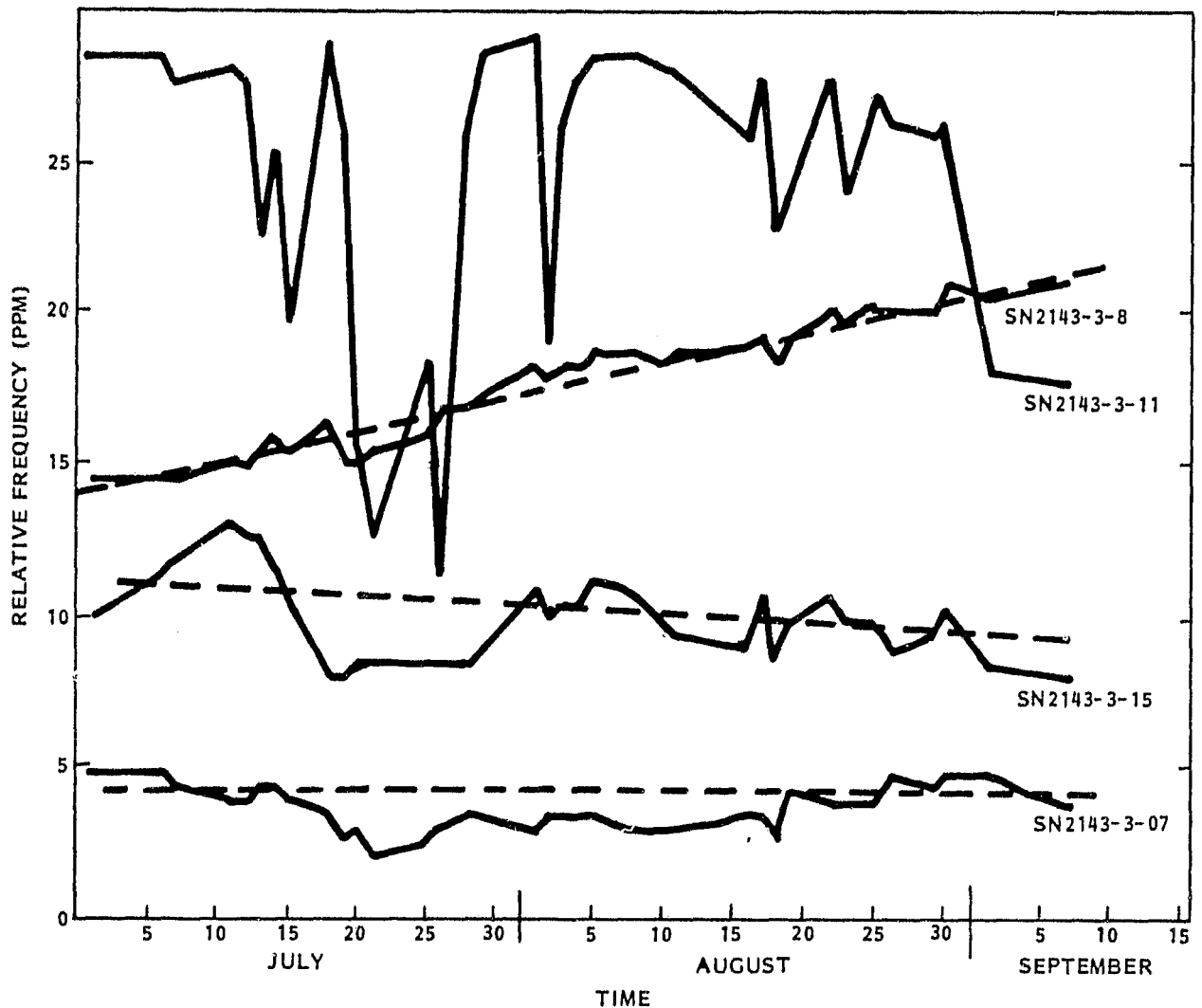


Figure 5-17. Results of Three-Month Aging Measurements of 4 2.144 GHz SBAW Oscillators

Since the aging rates are not consistent among oscillators, it is difficult to precisely identify the cause of aging. The only consistent trend of the data is that much higher aging rates were observed for the 2 GHz SBAW oscillator as compared to the 1 GHz SBAW oscillators. The probable cause of this is overdriving of SBAW transducers. The 2 GHz SBAW transducers are more susceptible to this effect because they contain fingers twice as narrow as the 1 GHz transducer and have a much thinner metal thickness.

## 6. REFERENCE SOURCE EVALUATION

The objective of the reference source evaluation task was to demonstrate the compatibility and improvement in performance of the SBAW oscillators in the circuits presently utilizing the surface acoustic wave (SAW) oscillator. Since the SBAW device is constructed similar to the SAW device, a direct replacement of the SAW device in a SAW oscillator circuit by a SBAW device is possible. The comparison of the 1 GHz SAW and SBAW devices was performed in this manner. The comparison of the 2 GHz SAW and SBAW devices presented somewhat of a problem because the 2 GHz SAW oscillator developed under NAS5-25095 was packaged in such a way that direct replacement of the SAW device by the SBAW device was not feasible. In this case, the comparison was made between SAW and SBAW oscillators constructed with different circuit components.

### 6.1 Comparison Between 1 GHz SAW and SBAW Oscillators

After termination of the 1 GHz SBAW oscillator aging study, one of the SBAW delay lines was removed from its oscillator circuit and replaced by a SAW delay line. The SAW delay line has performance parameters similar to that of the SBAW delay line it replaced. Its insertion loss was 25 dB and the time delay was 0.35  $\mu$ sec., approximately 20% shorter than that of the SBAW delay line. The phase noise and temperature stability comparison of the oscillators is shown in Table 6.1. The phase noise characteristics of the two oscillators are basically identical. The larger temperature shift in the SAW oscillator is due primarily to the fact that the turnover temperature of the device is  $-10^{\circ}\text{C}$ .

Table 6.1 1.07 GHz Oscillator Comparison

PARAMETER	SAWO	SBAWO
TEMPERATURE STABILITY ( $-20^{\circ}\text{C}$ to $+50^{\circ}\text{C}$ )	$\pm 75$ ppm	$\pm 47$ ppm
PHASE NOISE, dBc/Hz		
1 KHz OFFSET	-74	-74
1 MHz OFFSET	-134	-136
LONG-TERM STABILITY	N/A	$1 \times 10^{-7}$ pp day

## 6.2 Comparison Between 2 GHz SAW and SBAW Oscillator

The 2 GHz SAW oscillator developed under a previous contract NAS5-25095 used a SAW delay line fabricated on an  $\text{AlN}/\text{Al}_2\text{O}_3$  substrate in its oscillator loop. The comparison between the two oscillators is shown in Table 6.2. The SBAWO has much better temperature stability, and the phase noise characteristics are better due to the lower insertion loss of the SBAW device.

Table 6.2 2.14 GHz Oscillator Comparison

PARAMETER	SAWO	SBAWO
TEMPERATURE STABILITY, ppm (-20 C to +50 C)	$\pm 1200$	$\pm 42$
PHASE NOISE, dBc/Hz		
1 KHz OFFSET	-68	-70
1 MHz OFFSET	-136	-158
LONG TERM STABILITY	$2.25 \times 10^{-6}$ pp day	$1 \times 10^{-7}$ pp day

## 6.3 Trade-off Between 1 GHz and 2 GHz Reference Sources

Both the 1 GHz and 2 GHz SBAW oscillators have demonstrated superior performance over their SAW counterparts. For an application, such as a Ku band source, the 2 GHz SBAW oscillator has an advantage over the 1 GHz version because less multiplication will be required. This will result in lower circuit complexity and less power consumption. The phase noise of the 1 and 2 GHz SBAW oscillators is basically a function of the noise figure of the loop amplifier, and a comparison between Tables 6.1 and 6.2 shows that the 2 GHz oscillator is already slightly superior in this aspect. It should be noted that phase noise of the 1 GHz oscillator followed by a multiplier circuit will be greater than that from the 2 GHz oscillator.

## 7. FREQUENCY SELECTABILITY AND SETTABILITY

The conclusion of the Phase I study of the frequency selectability and settability was that up to  $\pm 21\%$  change in device center frequency is possible for a given mask design if the rotated Y cut angle of the substrate is properly chosen. Accompanying these frequency changes were variations in temperature coefficient of the device time delay. For smaller changes in frequency on a given substrate, approximately  $\pm 1\%$  could be realized by adjusting the metal film thickness of the SBAW transducer. A similar amount of frequency settability can be achieved by adjusting the phase in the oscillator loop.

The Phase II program continued this Phase I effort by designing a single mask and fabricating devices on five different cuts of singly rotated Y cut quartz substrates. The five target frequencies were 2287.5, 2230.0, 2208.0, 2116.0 and 2106.4 MHz. The following sections describe the approach and experimental results.

### 7.1 Analysis and Device Design

Based on design curves calculated during Phase I of the program and reproduced in Figure 7.1, it is evident that if the 2287.5 MHz device was fabricated on  $+35.5^\circ$  rotated Y cut quartz, the devices at the other frequencies must be fabricated on substrates whose rotated Y-cut angle,  $\theta$ , is somewhat larger than  $40^\circ$ . Table 7-1 summarizes the details of the theoretical analysis to select the desired substrate angle. The design of the mask for this study was based on the third harmonic design for the 2.144 GHz SBAW delay line described in Section 4.1. The transducer portion was simply scaled down by a factor which reduced the finger width from  $0.89 \mu\text{m}$  to  $0.836 \mu\text{m}$ .

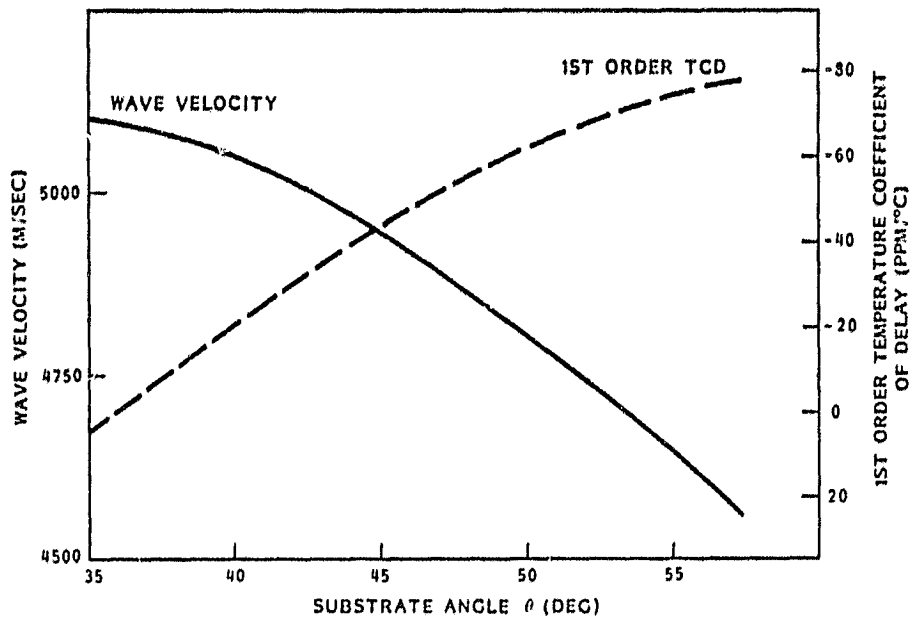


Figure 7-1. SBAW Velocity and First Order TCD as a Function of  $\theta$  in Rotated Y-Cut Quartz.

Table 7-1. Theoretical Calculations

TARGET FREQUENCY (MHz)	WAVELENGTH ( $\mu$ M)	CRYSTAL CUT ANGLE $\theta$ (DEG)	CALCULATED WAVE VELOCITY (M/SEC)
2287.5	2.226	35.5	5092
2230.0	2.226	44.0	4964
2208.0	2.226	46.2	4915
2116.0	2.226	53.4	4710
2106.4	2.226	54.0	4689

## 7.2 Data Summary

Approximately 5 devices on each substrate were fabricated using the mask whose designed finger width was 0.836  $\mu\text{m}$ . All devices were fabricated with embedded fingers. The embedded groove depth was approximately 350  $\text{\AA}$  and the aluminum metal thickness 400  $\text{\AA}$ . The measured center frequencies as summarized in Table 7.2 of these devices were generally 12-17 MHz lower than the target frequencies. A 0.5% error in mask line-width error was confirmed by laser interferometric measurements. There were, however, additional errors which amount to 0.1 or 0.2%. Such errors were attributed partly to fabrication errors such as finger/gap ratio variance and metal/groove depth variance. Additional errors were due to crystal angle uncertainties which could amount to 0.1% in frequency shift for a 15 minute angle error.

Table 7-2. Results of Frequency Settability Study

CRYSTAL ANGLES	TARGET FREQUENCY (MHz)	MEASURED FREQUENCY (MHz)	% OFF
35.5°	2287.5	2270.0 $\pm$ 2.9	0.77
44.0°	2230.0	2217.2 $\pm$ 1.5	0.58
46.2°	2208.0	2197.4 $\pm$ 2.5	0.48
53.4°	2116.0	2102.2 $\pm$ 1.0	0.65
54.0°	2106.4	2093.5 $\pm$ 1.7	0.61

One effect of this method of oscillator frequency selection is that the temperature stability of the oscillators deteriorates. To fully characterize this effect, the delay lines were placed in an oscillator loop and their temperature coefficient of delay measured. Table 7.3 summarizes the results of this measurement. Another effect which is a consequence

of changing the substrate angle  $\theta$  is a change in delay line insertion loss due to the change in the coupling constant. The typical unmatched loss for the delay lines is also included in Table 7.3. The results are in agreement with the theoretical predictions, except for the one insertion loss anomaly at  $\theta = 53.4^\circ$ ; this could be attributed to device imperfection.

Table 7-3. Insertion Loss and First Order TCD of SBAW Devices.

REFERENCE FREQUENCY GHz	$\theta$ DEGREES	TCD  ppm/ $^\circ$ C	UNMATCHED IL (dB)
2.270	+35.5	-2.0	22
2.217	+44.0	31.3	21
2.197	+46.2	38.5	16
2.101	+53.4	54.5	24
2.093	+54.0	58.5	21

ORIGINAL PAGE IS  
OF POOR QUALITY